AIMS Mathematics, 7(6): 9926–9956.
DOI: 10.3934/math.2022554
Received: 21 August 2021
Revised: 18 December 2021
Accepted: 17 January 2022
Published: 21 March 2022

http://www.aimspress.com/journal/Math

Research article

Estimation method of mixture distribution and modeling of COVID-19 pandemic

Tabassum Naz Sindhu[1,*], Zawar Hussain[2], Naif Alotaibi[3,*] and Taseer Muhammad[4]

1 Department of Statistics, Quaid-i-Azam University 45320, Islamabad 44000, Pakistan
2 Department of Social & Allied Sciences, Cholistan University of Veterinary & Animal Sciences, Bahawalpur 63100, Pakistan
3 Department of Mathematics and Statistics, Imam Mohammad Ibn Saud Islamic University, Kingdom of Saudi Arabia
4 Department of Mathematics, College of Sciences, King Khalid University, Abha 61413, Saudi Arabia

*** Correspondence:** Email: sindhuqau@gmail.com, nmaalotaibi@imamu.edu.sa.

Abstract: The mathematical characteristics of the mixture of Lindley model with 2-component (2-CMLM) are discussed. In this paper, we investigate both the practical and theoretical aspects of the 2-CMLM. We investigate several statistical features of the mixed model like probability generating function, cumulants, characteristic function, factorial moment generating function, mean time to failure, Mills Ratio, mean residual life. The density, hazard rate functions, mean, coefficient of variation, skewness, and kurtosis are all shown graphically. Furthermore, we use appropriate approaches such as maximum likelihood, least square and weighted least square methods to estimate the pertinent parameters of the mixture model. We use a simulation study to assess the performance of suggested methods. Eventually, modelling COVID-19 patient data demonstrates the effectiveness and utility of the 2-CMLM. The proposed model outperformed the two component mixture of exponential model as well as two component mixture of Weibull model in practical applications, indicating that it is a good candidate distribution for modelling COVID-19 and other related data sets.

Keywords: mixture model; least square estimation, Mills Ratio, weighted least square estimation
Mathematics Subject Classification: 62E10, 62E15, 62F10

Symbols

$f(t\|\breve{\Delta})$	PDF	$F(t\|\breve{\Delta})$	CDF
$R(t\|\breve{\Delta})$	RF	$h(t\|\breve{\Delta})$	HRF
$H(t\|\breve{\Delta})$	CHRF	$Q(q;\breve{\Delta})$	QF
$\Upsilon\left(t\|\breve{\Delta}\right)$	Mills Ratio	$R\left(t\|\breve{\Delta}\right)$	RF
$\tilde{M}_t(\upsilon)$	MGF	$\breve{\xi}_t(\upsilon)$	CF
$P_t(\omega)$	PGF	$\breve{F}_t(\omega)$	FMGF
$\breve{K}(\upsilon)$	CGF	$h\left(t\|\breve{\Delta}\right)$	RHRF
$\breve{M}\left(t\|\breve{\Delta}\right)$	MTTF	$\breve{M}_R\left(t\|\breve{\Delta}\right)$	MRL

Abbreviations

PDF	Probability Density Function	TTF	Time-To-Failure
CDF	Cumulative Distribution Function	QF	Quantile Function
PGF	Probability Generating Function	MTTF	Mean Time to Failure
MLE	Maximum Likelihood Estimator	HRF	Hazard Rate Function
FMGF	Factorial Moment Generating Function	MSE	Mean Square Error
MGF	Moment Generating Function	CF	Characteristic Function
RHRF	Reversed Hazard Rate Function	LSE	Least Square Estimator
WLSE	Weighted Least Square Estimator	MRL	Mean Residual Life
CGF	Cumulant Generating Function	MGF	Moment Generating Function
CHRF	Cumulative Hazard Rate Function	RF	Reliability Function

1. Introduction

In the early days of statistics, mixture models, specifically finite mixture models, were employed to simulate a variety of events, and their use has grown through time. In many scenarios, available data can be seen as a mixture of two or more distributions. We can merge statistical distributions using this notion to create a new one. Finite mixture models are useful in a variety of domains, including biology, engineering, genetics, healthcare, business, marketing, real life, and social sciences. The basic concept behind mixture models is to combine two or more models by adjusting proportions to produce a novel model with new attributes. As a result, it's crucial to investigate the statistical features of the proposed mixture model and use appropriate methods to estimate its unknown parameters. Finite mixture densities can be used to model data from populations known or suspected to contain a number of separate subpopulations. Most commonly used are mixture densities with Gaussian components, but mixtures with other types of component are also increasingly used to model, for example, survival times. Mixing distributions have been studied by several writers, including [1–5]. The classical features of the mixture of Burr XII and Weibull distribution were investigated by Muhammad and Muhammad [6]. Sultan et al. [7] suggested a 2-Component Mixture of Inverse Weibull models (2-CMIWD) and investigated some of its features using density and hazard function graphs. To examine the hybrid of two inverse Weibull distributions, Jiang et al. [8] focused at the forms of the PDF and hrfs as well as graphical approaches. The following are several authors who deal with mixture modeling in different practical problems: Mohammadi et al. [9], Ateya [10], Mohamed et al. [11], and Sindhu et al. [12]. Some other relevant studies are [13–19].

Because of its practical application, the Lindley model, which belongs to the family of exponential models, is important. Lindley model is useful for modelling many types of life time and reliability data. The Lindley distribution has captivated the curiosity of scholars in recent years. The generalized Lindley (GL), model was introduced by Zakerzadah and Dolati [20], who studied its statistical content and capabilities. A new class of GL models was suggested by Oluyede and Yang [21] and Nadarajah et al. [22]. The researchers [23] developed the Lindley model to illustrate the distinction between Fiducial and subsequent models in the perspective of Fiducial and Bayesian statistics. Furthermore, [24] discusses the statistical features of Lindley models, demonstrating that this model is a superior model for particular application than other models like the exponential model. When modelling various lifetime data sets, Shanker, et al. [25] used the Lindley model. Mazucheli and Achcar [26] demonstrated that the Lindley model may be used to describe strength data effectively, and they recommended it as a suitable alternative to the exponential and Weibull distributions. Furthermore, by adding another shape parameter to the model and naming it a power Lindley model, [27] developed a new extension of the Lindley model. [28,29] investigated a mixture of Lindley models from different perspectives.

Al-Moisheer et al. [30] examined mixture of Lindley models and used ML and the generalized method of moments to evaluate the unknown parameters of the mixture model. Besides that, it is interesting to compare the MLE method to other estimation techniques such as least-squares estimation (LSE), weighted least-squares estimation (WLSE), and other methods of estimation. In the literature, there are various estimating methods for parametric distributions, some of which have been widely investigated from a theoretical perspective. It is worth mentioning, too, that in the case of small n the maximum likelihood method frequently fails. As a consequence, new estimation

techniques have recently been suggested. The usefulness of estimating methods varies depending on the user and the application area. For example, even though the moment estimator does not have a closed form expression, it may be preferable to utilize it. The goal of this paper is to provide framework for selecting the optimum estimation technique for the 2-Component Mixture of Lindley Model (2-CMLM) distribution that would be useful to professional statisticians. In this study, we use least square estimation (LSE) and weighted least square estimation (WLSE), in addition to MLE, to estimate the 2-Component Mixture of Lindley Model (2-CMLM). In the literature, analyses of estimation methods for other distributions have been examined, for example, [31–35].

This study has two key objectives: The first is to demonstrate how various frequentist estimators of the proposed distribution perform for different sample sizes and different parametric values. The second step is to investigate some additional model attributes and demonstrate that the distribution outperforms its competitor mixed model with two real data sets.

2. The 2-component mixture of Lindley model (2-CMLM)

A random variable T is said to have a finite mixture of Lindley model with 2-component (2-CMLM) if it's PDF and CDF can be composed as:

$$f\left(t|\ \breve{\Delta}\right)=\pi f_1\left(t|\ \vartheta_1\right)+\breve{\pi} f_2\left(t|\ \vartheta_2\right), \breve{\pi}=1-\pi \tag{1}$$

$$f\left(t|\ \breve{\Delta}\right)=\pi\frac{\vartheta_1^2}{\vartheta_1+1}(1+t)\exp\left(-\vartheta_1 t\right)+\breve{\pi}\frac{\vartheta_2^2}{\vartheta_2+1}(1+t)\exp\left(-\vartheta_2 t\right), \tag{2}$$

and

$$F\left(t|\ \breve{\Delta}\right)=\pi F_1\left(t|\ \vartheta_1\right)+\breve{\pi} F_2\left(t|\ \vartheta_2\right), \tag{3}$$

$$F\left(t|\ \breve{\Delta}\right)=\pi\left\{1-\frac{\vartheta_1+1+\vartheta_1 t}{\vartheta_1+1}\exp\left(-\vartheta_1 t\right)\right\}+\breve{\pi}\left\{1-\frac{\vartheta_2+1+\vartheta_2 t}{\vartheta_2+1}\exp\left(-\vartheta_2 t\right)\right\}, \tag{4}$$

where $\breve{\Delta}=\left(\vartheta_1,\vartheta_2,\pi\right)$ are the positive scale parameters, while π is positive mixing parameter.

Figure 1 shows several graphs of $f\left(t|\breve{\Delta}\right)$ and both density for various parameter values. The PDF demonstrates how the parametric vector $\left(\breve{\Delta}\right)$ alters the density of 2-CMLM$\left(\breve{\Delta}\right)$. We may point out that the values for parameters were chosen randomly until a variety of shapes could be captured. The 2-CMLM$\left(\breve{\Delta}\right)$ can be right skewed as shown in Figure 1.

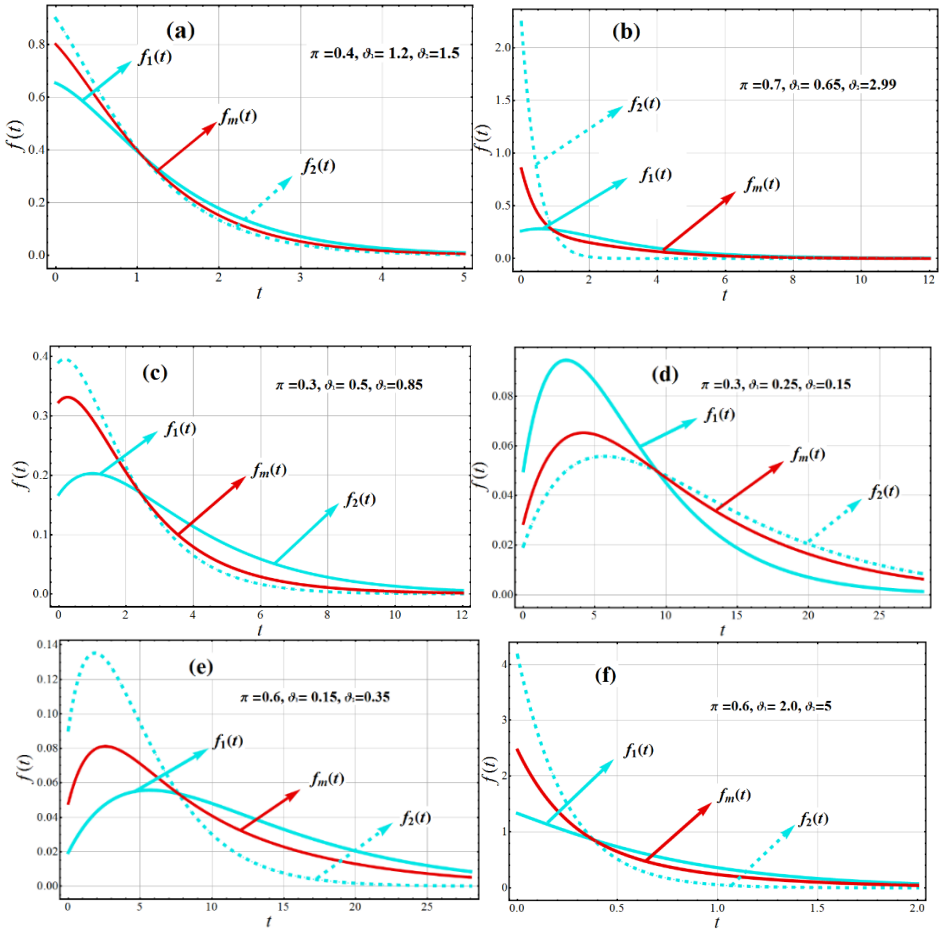

Figure 1. Variations of first component density $f_1(t)$, second component density $f_2(t)$ and density of 2-CMLM $f_m\left(t|\breve{\Delta}\right)$.

2.1. Mode

The mode of the 2-CMLM $\left(\breve{\Delta}\right)$ is obtained by solving the following nonlinear equation with respect to t:

$$\pi\frac{\vartheta_1^2}{\vartheta_1+1}\left\{\exp\left(-\vartheta_1 t\right)-\left(1+t\right)\vartheta_1\exp\left(-\vartheta_1 t\right)\right\}+\breve{\pi}\frac{\vartheta_2^2}{\vartheta_2+1}\left\{\exp\left(-\vartheta_2 t\right)-\left(1+t\right)\vartheta_2\exp\left(-\vartheta_2 t\right)\right\}=0. \quad (5)$$

2.2. Median

The median of 2-CMEM $\left(\breve{\Delta}\right)$ is presented here. Suppose that $F\left(t|\breve{\Delta}\right)$ be the CDF of 2-CMLM $\left(\breve{\Delta}\right)$ Model at 0.5$^{\text{th}}$ quantile $Q_{0.5}$. Then by solving the following non-linear equation for t, one may get the median $\left(t^*\right)$.

$$\pi\left\{1-\frac{\vartheta_1+1+\vartheta_1 t}{\vartheta_1+1}\exp\left(-\vartheta_1 t\right)\right\}+\breve{\pi}\left\{1-\frac{\vartheta_2+1+\vartheta_2 t}{\vartheta_2+1}\exp\left(-\vartheta_2 t\right)\right\}=0.5 \quad (6)$$

$$\pi\left\{\frac{\vartheta_1+1+\vartheta_1 t}{\vartheta_1+1}\exp\left(-\vartheta_1 t\right)\right\}+\breve{\pi}\left\{\frac{\vartheta_2+1+\vartheta_2 t}{\vartheta_2+1}\exp\left(-\vartheta_2 t\right)\right\}=0.5 \tag{7}$$

For the determination of t^* (median) from Eq (7) computational algorithms like Newton-Raphson techniques can be used.

Various graphs of $h\left(t|\breve{\Delta}\right)$ for various parameter values are shown in Figure 2. The density of 2-CMLM$\left(\breve{\Delta}\right)$ is influenced by the parametric vector$\left(\breve{\Delta}\right)$, as shown in the Figure 2. It's worth noting that parameter values were chosen at random until a range of shapes could be captured. The HRF of each component distribution shows growing activity, while the HRF of 2-CMLM $\left(\breve{\Delta}\right)$ shows obvious increasing and decreasing behavior, as shown in the figure.

Graphs of the mean of 2-CMLM$\left(\breve{\Delta}\right)$for various parameter values may be found in Figure 3. It is worth noting that parameter values were chosen at random until a wide range of shapes could be captured. The mean of each component distribution, as well as 2-CMLM$\left(\breve{\Delta}\right)$, shows a decreasing and constant pattern. Also the 3D Variations of Mean of 2-CMLM $\left(\breve{\Delta}\right)$ is observed in Figure 4 and mean decrease as ϑ_2 increases, as illustrated in this graph.

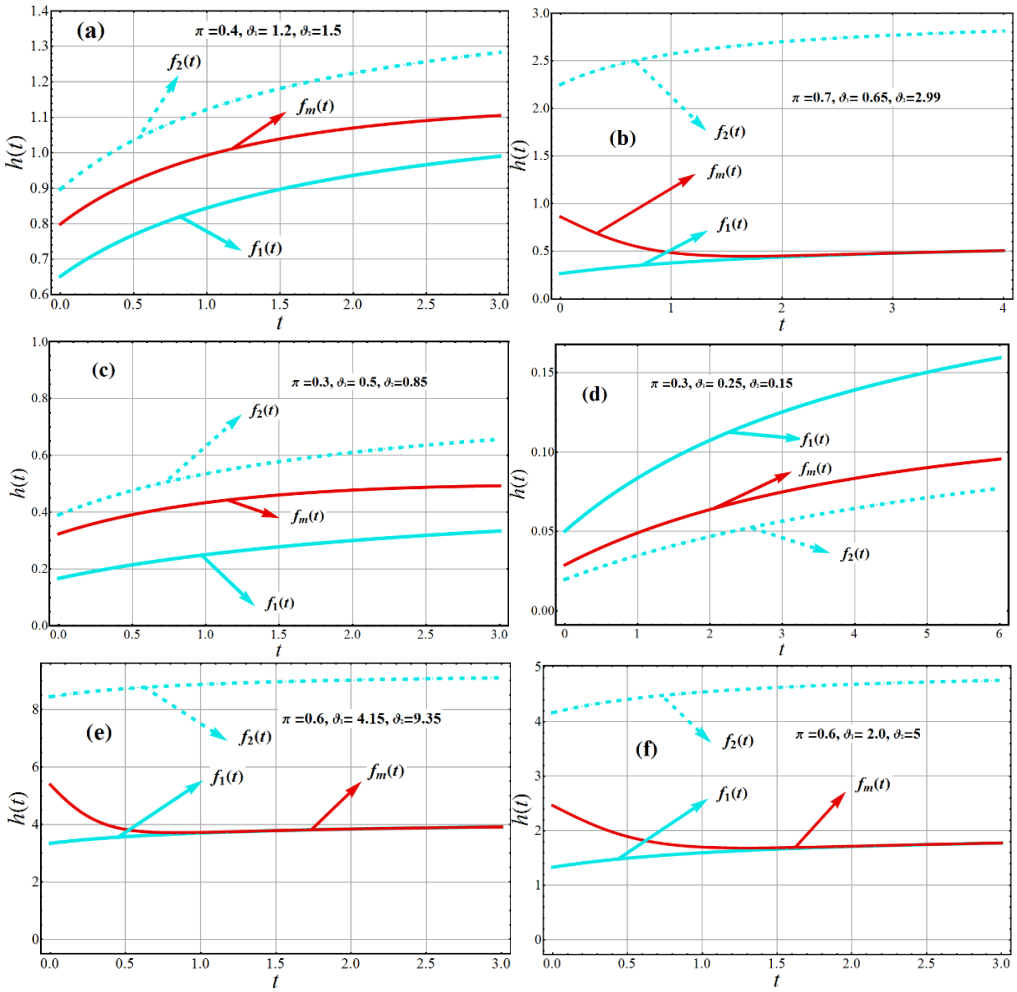

Figure 2. Variations of $h\left(t|\breve{\Delta}\right)$ of 2-CMLM$\left(\breve{\Delta}\right)$.

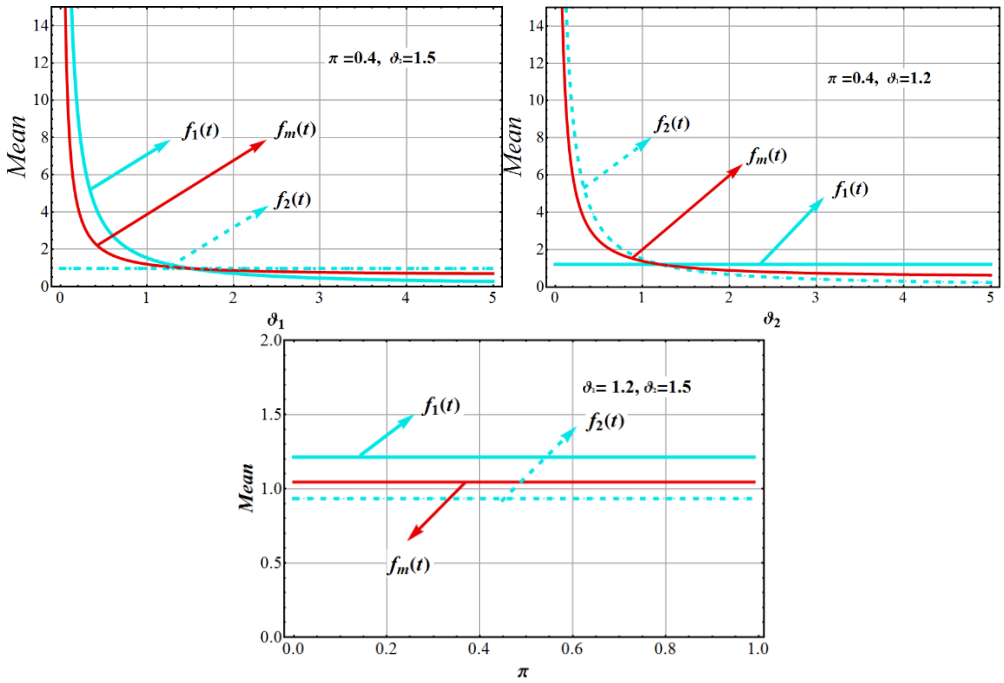

Figure 3. Variations of Mean of 2-CMLM $\left(\breve{\Delta}\right)$.

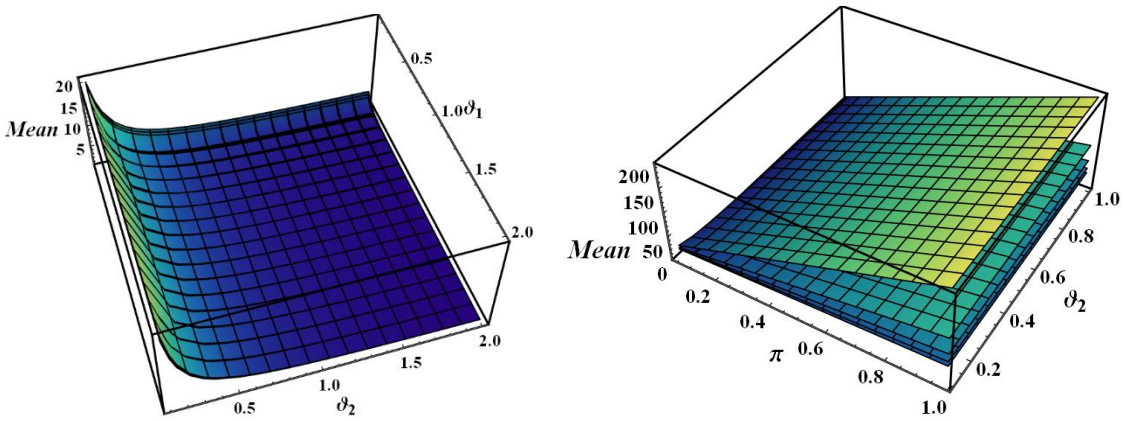

Figure 4. 3D Variations of Mean of 2-CMLM $\left(\breve{\Delta}\right)$.

2.3. m^{th} moments about origin

For a random variable T, the m^{th} moments about the origin of a 2-CMLM $\left(\breve{\Delta}\right)$ are as follows:

$$\breve{\mu}_m = E\left(T^m\right) = \int_0^\infty t^m f\left(t|\ \breve{\Delta}\right)dt = \int_0^\infty t^m \left\{\pi \frac{\vartheta_1^2}{\vartheta_1+1}(1+t)\exp\left(-\vartheta_1 t\right) + \breve{\pi}\frac{\vartheta_2^2}{\vartheta_2+1}(1+t)\exp\left(-\vartheta_2 t\right)\right\}dt, \qquad (8)$$

$$E\left(T^m\right)=\pi\frac{m!\left(\vartheta_1+m+1\right)}{\vartheta_1^m\left(\vartheta_1+1\right)}+\breve{\pi}\frac{m!\left(\vartheta_2+m+1\right)}{\vartheta_2^m\left(\vartheta_2+1\right)},m=1,2.... \tag{9}$$

The mean of the PDF of the 2-CMLM $\left(\breve{\Delta}\right)$ is:

$$\breve{\mu}_1=\pi\frac{\left(\vartheta_1+2\right)}{\vartheta_1\left(\vartheta_1+1\right)}+\breve{\pi}\frac{\left(\vartheta_2+2\right)}{\vartheta_2\left(\vartheta_2+1\right)}=\mu, \tag{10}$$

while the variance is given by

$$\breve{\sigma}=\pi\frac{\left(\vartheta_1^2+4\vartheta_1+2\right)}{\vartheta_1^2\left(\vartheta_1+1\right)^2}+\breve{\pi}\frac{\left(\vartheta_2^2+4\vartheta_2+2\right)}{\vartheta_2^2\left(\vartheta_2+1\right)^2}. \tag{11}$$

In particular first four moments about origin

$$\breve{\mu}_1=\pi\frac{\left(\vartheta_1+2\right)}{\vartheta_1\left(\vartheta_1+1\right)}+\breve{\pi}\frac{\left(\vartheta_2+2\right)}{\vartheta_2\left(\vartheta_2+1\right)}, \tag{12}$$

$$\breve{\mu}_2=\pi\frac{2\left(\vartheta_1+3\right)}{\vartheta_1^2\left(\vartheta_1+1\right)}+\breve{\pi}\frac{2\left(\vartheta_2+3\right)}{\vartheta_2^2\left(\vartheta_2+1\right)}, \tag{13}$$

$$\breve{\mu}_3=\pi\frac{6\left(\vartheta_1+4\right)}{\vartheta_1^3\left(\vartheta_1+1\right)}+\breve{\pi}\frac{6\left(\vartheta_2+4\right)}{\vartheta_2^3\left(\vartheta_2+1\right)}, \tag{14}$$

$$\breve{\mu}_4=\pi\frac{24\left(\vartheta_1+5\right)}{\vartheta_1^4\left(\vartheta_1+1\right)}+\breve{\pi}\frac{24\left(\vartheta_2+5\right)}{\vartheta_2^4\left(\vartheta_2+1\right)}, \tag{15}$$

and the central moments of the 2-CMLM $\left(\breve{\Delta}\right)$ are:

$$\mu_2=\pi\frac{\left(\vartheta_1^2+4\vartheta_1+2\right)}{\vartheta_1^2\left(\vartheta_1+1\right)^2}+\breve{\pi}\frac{\left(\vartheta_2^2+4\vartheta_2+2\right)}{\vartheta_2^2\left(\vartheta_2+1\right)^2}, \tag{16}$$

$$\mu_3=\pi\frac{2\left(\vartheta_1^3+6\vartheta_1^2+6\vartheta_1+2\right)}{\vartheta_1^3\left(\vartheta_1+1\right)^3}+\breve{\pi}\frac{2\left(\vartheta_2^3+6\vartheta_2^2+6\vartheta_2+2\right)}{\vartheta_2^3\left(\vartheta_2+1\right)^3}, \tag{17}$$

$$\mu_4=\pi\frac{3\left(3\vartheta_1^4+24\vartheta_1^3+44\vartheta_1^2+32\vartheta_1+8\right)}{\vartheta_1^4\left(\vartheta_1+1\right)^4}+\breve{\pi}\frac{3\left(3\vartheta_2^4+24\vartheta_2^3+44\vartheta_2^2+32\vartheta_2+8\right)}{\vartheta_2^4\left(\vartheta_2+1\right)^4}. \tag{18}$$

The Coefficient of Variation $\left(\breve{\varphi}_{CV}\right)$, Skewness $\left(\breve{\Psi}_{Sk}\right)$ and the Kurtosis $\left(\breve{\psi}_K\right)$ of the 2-CMLM $\left(\breve{\Delta}\right)$ are:

$$\breve{\varphi}_{CV} = \pi \frac{\sqrt{\left(\vartheta_1^2 + 4\vartheta_1 + 2\right)}}{\left(\vartheta_1 + 2\right)} + \breve{\pi} \frac{\sqrt{\left(\vartheta_2^2 + 4\vartheta_2 + 2\right)}}{\left(\vartheta_2 + 2\right)} \tag{19}$$

$$\Psi_{Sk} = \pi \frac{2\left(\vartheta_1^3 + 6\vartheta_1^2 + 6\vartheta_1 + 2\right)}{\left(\vartheta_1^2 + 4\vartheta_1 + 2\right)^{3/2}} + \breve{\pi} \frac{2\left(\vartheta_2^3 + 6\vartheta_2^2 + 6\vartheta_2 + 2\right)}{\left(\vartheta_2^2 + 4\vartheta_2 + 2\right)^{3/2}}, \tag{20}$$

and

$$\breve{\psi}_K = \pi \frac{3\left(3\vartheta_1^4 + 24\vartheta_1^3 + 44\vartheta_1^2 + 32\vartheta_1 + 8\right)}{\left(\vartheta_1^2 + 4\vartheta_1 + 2\right)^2} + \breve{\pi} \frac{3\left(3\vartheta_2^4 + 24\vartheta_2^3 + 44\vartheta_2^2 + 32\vartheta_2 + 8\right)}{\left(\vartheta_2^2 + 4\vartheta_2 + 2\right)^2}. \tag{21}$$

The graphs of Coefficient of Variation of 2-CMLM $\left(\breve{\Delta}\right)$ for various parameter values are shown in Figure 5. It's interesting to note that parameter values were randomly chosen until a range of shapes could be captured. The Coefficient of Variation of each component distribution increases and remains constant as the Coefficient of Variation of 2-CMLM $\left(\breve{\Delta}\right)$ increases.

Figure 6 depicts the graphs of the Coefficient of Skewness 2-CMLM $\left(\breve{\Delta}\right)$ for various parameter values. As seen in Figure 6, the Skewness Coefficient of each component distribution and 2-CMLM $\left(\breve{\Delta}\right)$ grows and remains constant. Figure 7 shows the increasing and constant behavior of the Coefficient of Kurtosis of each component distribution, as well as the decreasing and increasing behavior of 2-CMLM $\left(\breve{\Delta}\right)$.

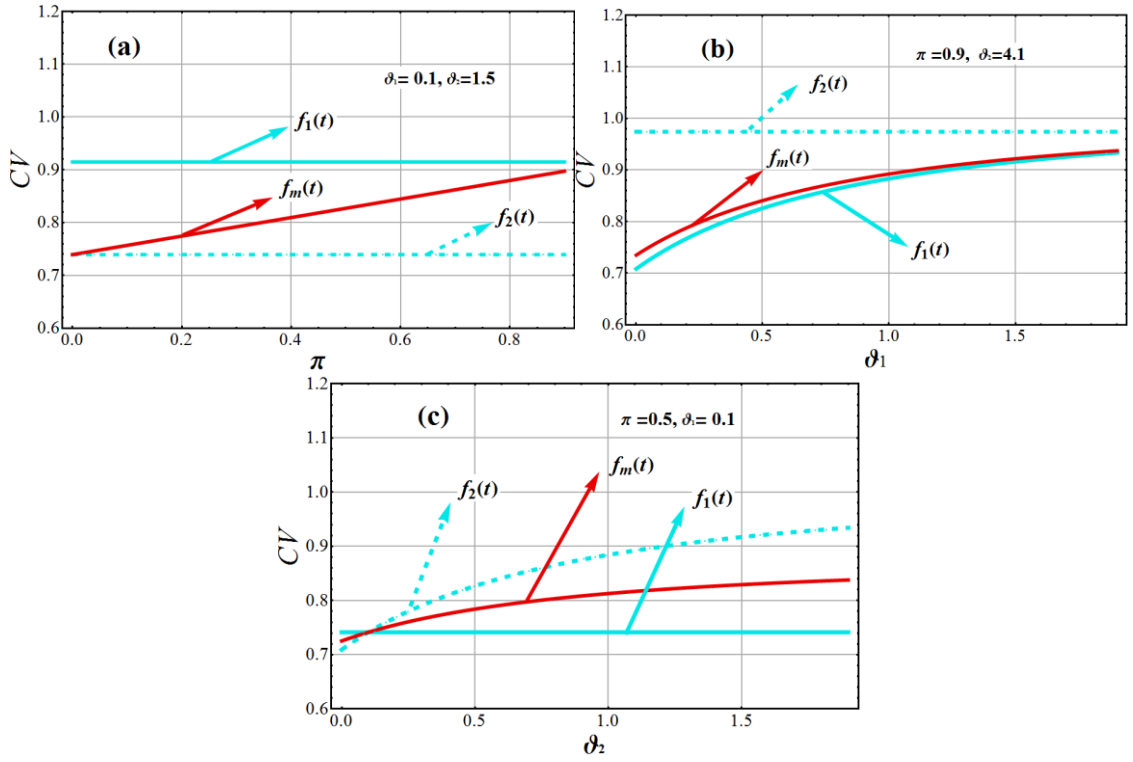

Figure 5. Variations of Coefficient of Variation $\left(\breve{\varphi}_{CV}\right)$ of 2-CMLM $\left(\breve{\Delta}\right)$.

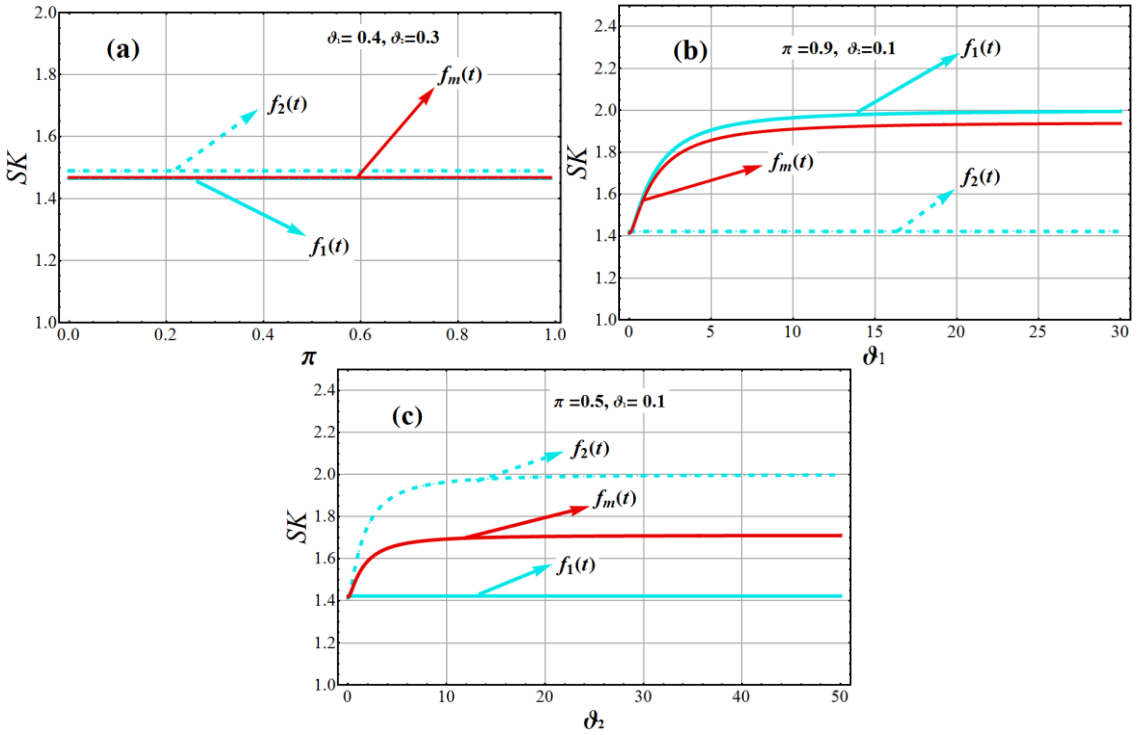

Figure 6. Variations of Coefficient of Skewness $\left(\breve{\Psi}_{Sk}\right)$ of 2-CMLM $\left(\breve{\Delta}\right)$.

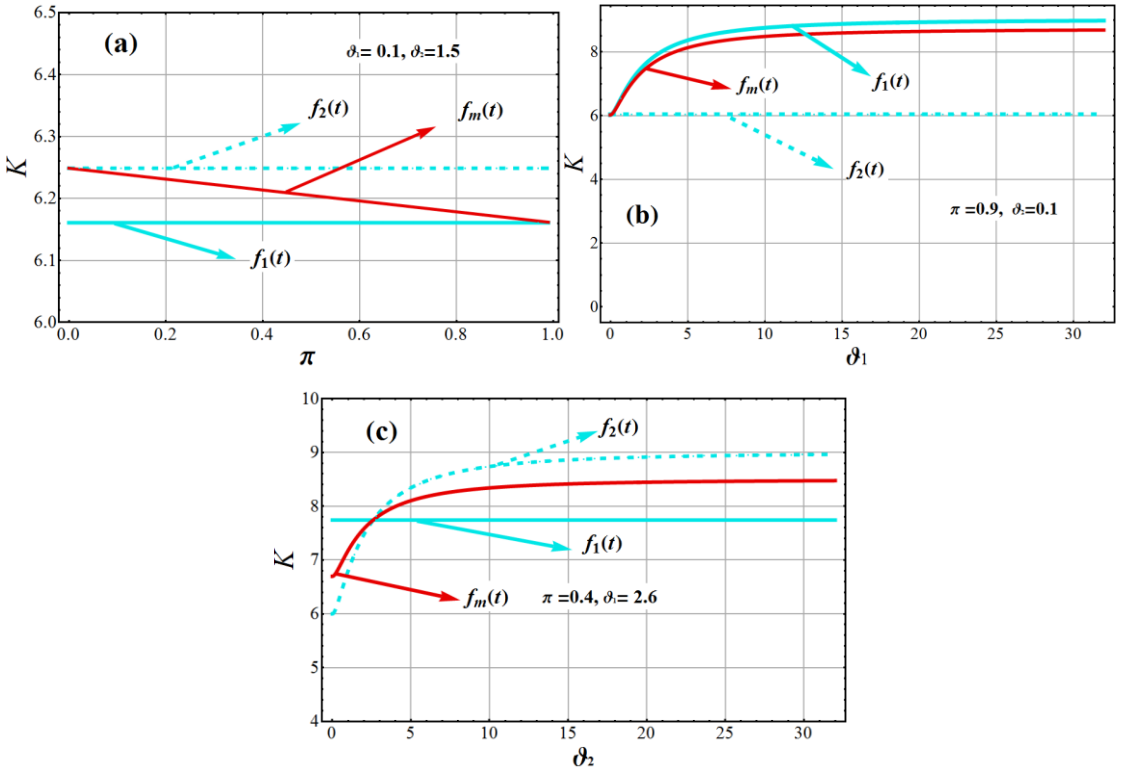

Figure 7. Variations of Coefficient of Kurtosis $\left(\breve{\psi}_K\right)$ of 2-CMLM $\left(\breve{\Delta}\right)$

2.4. Moment Generating Function (MGF)

The MGF of 2-CMLM $\left(\breve{\Delta}\right)$ is specified as:

$$\tilde{M}_t(\upsilon)=E\left(e^{t\upsilon}\right)=\int_0^{\infty}e^{t\upsilon}\left\{\pi\frac{\vartheta_1^2}{\vartheta_1+1}(1+t)\exp(-\vartheta_1 t)+\breve{\pi}\frac{\vartheta_2^2}{\vartheta_2+1}(1+t)\exp(-\vartheta_2 t)\right\}dt, \tag{22}$$

$$\tilde{M}_t(\upsilon)=\pi\frac{\vartheta_1^2(\vartheta_1-\upsilon+1)}{(\vartheta_1+1)(\vartheta_1-\upsilon)^2}+\breve{\pi}\frac{\vartheta_2^2(\vartheta_2-\upsilon+1)}{(\vartheta_2+1)(\vartheta_2-\upsilon)^2}. \tag{23}$$

2.5. Cumulants

The characteristic function (CF), $\breve{\xi}(\upsilon)=E\left[\exp(i\upsilon t)\right]$ of 2-CMLM $\left(\breve{\Delta}\right)$ is obtained by substituting υ with '$i\upsilon$' in Eq (22), the CF can be determined as

$$\breve{\xi}(\upsilon)=\pi\frac{\vartheta_1^2(\vartheta_1-i\upsilon+1)}{(\vartheta_1+1)(\vartheta_1-i\upsilon)^2}+\breve{\pi}\frac{\vartheta_2^2(\vartheta_2-i\upsilon+1)}{(\vartheta_2+1)(\vartheta_2-i\upsilon)^2}, \tag{24}$$

where $i=\sqrt{-1}$ is the complex unit.

2.6. Cumulant Generating Function (CGF)

The cumulant generating function (CGF) is $\log\left(\breve{\xi}(\upsilon)\right)$

$$\breve{K}(\upsilon)=\pi\left\{\log\left(1-\frac{i\upsilon}{\vartheta_1+1}\right)-2\log\left(1-\frac{i\upsilon}{\vartheta_1}\right)\right\}+\breve{\pi}\left\{\log\left(1-\frac{i\upsilon}{\vartheta_2+1}\right)-2\log\left(1-\frac{i\upsilon}{\vartheta_2}\right)\right\} \tag{25}$$

2.7. Probability Generating Function (PGF)

In Eq (22), we can get the PGF by substituting υ with $\ln(\omega)$ as follows:

$$P_t(\omega)=E\left(\omega^t\right)=E\left(e^{t\ln\omega}\right)=\pi\frac{\vartheta_1^2(\vartheta_1-\ln(\omega)+1)}{(\vartheta_1+1)(\vartheta_1-\ln(\omega))^2}+\breve{\pi}\frac{\vartheta_2^2(\vartheta_2-\ln(\omega)+1)}{(\vartheta_2+1)(\vartheta_2-\ln(\omega))^2}. \tag{26}$$

2.8. Factorial Moment Generating Function (FMGF)

By substituting υ with '$\ln(1+\phi)$' in Eq (22), the FMGF can be determined as

$$\breve{F}_t(\omega)=E\left(e^{t\ln(1+\phi)}\right)=\pi\frac{\vartheta_1^2(\vartheta_1-\ln(1+\phi)+1)}{(\vartheta_1+1)(\vartheta_1-\ln(1+\phi))^2}+\breve{\pi}\frac{\vartheta_2^2(\vartheta_2-\ln(1+\phi)+1)}{(\vartheta_2+1)(\vartheta_2-\ln(1+\phi))^2}. \tag{27}$$

3. Reliability measures

The reliability function /survival function and failure rate /hazard rate function are used to classify lifespan models in reliability theory. A ratio of the lifespan model to the reliability function is the hazard rate function. If the dependability function's value is lower, it indicates that the item or component has a shorter lifespan, then the hazard rate will be larger, which means the likelihood of failure will be higher. On the other hand, a higher reliability function value means a lower hazard rate, which means a lesser risk of failure. The reliability properties of 2-CMLM $\left(\breve{\Delta}\right)$ are now being investigated.

3.1. Reliability function

The reliability function /survival function $R\left(t|\ \breve{\Delta}\right)$ of 2-CMLM $\left(\breve{\Delta}\right)$ is.

$$R\left(t|\ \breve{\Delta}\right)=\pi\frac{\vartheta_1+1+\vartheta_1 t}{\vartheta_1+1}\exp\left(-\vartheta_1 t\right)+\breve{\pi}\frac{\vartheta_2+1+\vartheta_2 t}{\vartheta_2+1}\exp\left(-\vartheta_2 t\right) \tag{28}$$

3.2. Hazard function

The following is the description of the failure rate function $h\left(t|\breve{\Delta}\right)$ (also known as the hazard rate function) of 2-CMLM$\left(\breve{\Delta}\right)$

$$h\left(t|\breve{\Delta}\right)=\frac{\pi\frac{\vartheta_1^2}{\vartheta_1+1}\left(1+t\right)\exp\left(-\vartheta_1 t\right)+\breve{\pi}\frac{\vartheta_2^2}{\vartheta_2+1}\left(1+t\right)\exp\left(-\vartheta_2 t\right)}{\pi\frac{\vartheta_1+1+\vartheta_1 t}{\vartheta_1+1}\exp\left(-\vartheta_1 t\right)+\breve{\pi}\frac{\vartheta_2+1+\vartheta_2 t}{\vartheta_2+1}\exp\left(-\vartheta_2 t\right)}. \tag{29}$$

3.3. Mills Ratio

Mills Ratio is a unique technique to describing reliability because of its connection to failure rate.

$$\Upsilon\left(t|\ \breve{\Delta}\right)=\frac{R\left(t|\ \breve{\Delta}\right)}{f\left(t|\ \breve{\Delta}\right)}=\frac{\pi\frac{\vartheta_1+1+\vartheta_1 t}{\vartheta_1+1}\exp\left(-\vartheta_1 t\right)+\breve{\pi}\frac{\vartheta_2+1+\vartheta_2 t}{\vartheta_2+1}\exp\left(-\vartheta_2 t\right)}{\pi\frac{\vartheta_1^2}{\vartheta_1+1}\left(1+t\right)\exp\left(-\vartheta_1 t\right)+\breve{\pi}\frac{\vartheta_2^2}{\vartheta_2+1}\left(1+t\right)\exp\left(-\vartheta_2 t\right)}. \tag{30}$$

3.4. Cumulative hazard rate function

The cumulative hazard rate function of 2-CMLM $\left(\breve{\Delta}\right)$ is

$$H\left(t|\ \breve{\Delta}\right)=\int_0^t h\left(y|\ \breve{\Delta}\right)dy=-\log\left[R\left(t|\ \breve{\Delta}\right)\right]. \tag{31}$$

It is a measure of risk: the higher the $H\left(t|\ \breve{\Delta}\right)$ value, the higher the risk of failure by *t*-time. It is noted that

$$R\left(t|\breve{\Delta}\right)=e^{-H\left(t|\breve{\Delta}\right)} \text{ and } f\left(t|\breve{\Delta}\right)=h\left(t|\breve{\Delta}\right)e^{-H\left(t|\breve{\Delta}\right)}. \tag{32}$$

Therefore,

$$H\left(t|\breve{\Delta}\right)=-\log\left[\pi\frac{\vartheta_1+1+\vartheta_1 t}{\vartheta_1+1}\exp\left(-\vartheta_1 t\right)+\breve{\pi}\frac{\vartheta_2+1+\vartheta_2 t}{\vartheta_2+1}\exp\left(-\vartheta_2 t\right)\right]. \tag{33}$$

3.5. Reversed hazard rate function

The ratio between the life likelihood function and its distribution function is defined as the reversed hazard rate of a random life.

$$\breve{h}\left(t|\breve{\Delta}\right)=\frac{f\left(t|\breve{\Delta}\right)}{F\left(t|\breve{\Delta}\right)}=\frac{\pi\frac{\vartheta_1^2}{\vartheta_1+1}\left(1+t\right)\exp\left(-\vartheta_1 t\right)+\breve{\pi}\frac{\vartheta_2^2}{\vartheta_2+1}\left(1+t\right)\exp\left(-\vartheta_2 t\right)}{1-\pi\left\{\frac{\vartheta_1+1+\vartheta_1 t}{\vartheta_1+1}\exp\left(-\vartheta_1 t\right)\right\}-\breve{\pi}\left\{\frac{\vartheta_2+1+\vartheta_2 t}{\vartheta_2+1}\exp\left(-\vartheta_2 t\right)\right\}}. \tag{34}$$

3.6. Mean Time to Failure (MTTF)

The expected (or average) time for which the device functions satisfactorily is given by the mean time to failure (MTTF). If 2-CMLM $\left(\breve{\Delta}\right)$ then reliability function is used to express MTTF, which is as follows:

$$\breve{M}\left(t|\breve{\Delta}\right)=\int_0^{+\infty}R\left(t|\breve{\Delta}\right)dt, \tag{35}$$

where $R(t)$ is given in Eq (28). Hence

$$\breve{M}\left(t|\breve{\Delta}\right)=\pi\frac{\left(\vartheta_1+2\right)}{\vartheta_1\left(\vartheta_1+1\right)}+\breve{\pi}\frac{\left(\vartheta_2+2\right)}{\vartheta_2\left(\vartheta_2+1\right)}. \tag{36}$$

3.7. Mean Residual Life (MRL)

Reliabilists, statisticians, survival analysts, and others have investigated the mean residual lifetime (MRL). It has given many of valuable results. The remaining lifetime after t for a component or system of age t is random. The mean residual life or mean remaining life is the expected value of this random residual lifetime and is denoted by $\breve{M}_R\left(t|\breve{\Delta}\right)$.

$$\breve{M}_R\left(t|\breve{\Delta}\right)=\frac{1}{R\left(t|\breve{\Delta}\right)}\int_t^{+\infty}R(x|\ \breve{\Delta})dx, \tag{37}$$

$$\breve{M}_R\left(t|\breve{\Delta}\right)=\frac{\left\{\frac{\pi\left(\vartheta_1+2+\vartheta_1 t\right)\exp\left(-\vartheta_1 t\right)}{\vartheta_1\left(\vartheta_1+1\right)}+\frac{\bar{\pi}\left(\vartheta_2+2+\vartheta_2 t\right)\exp\left(-\vartheta_2 t\right)}{\vartheta_2\left(\vartheta_2+1\right)}\right\}}{\pi\frac{\vartheta_1+1+\vartheta_1 t}{\vartheta_1+1}\exp\left(-\vartheta_1 t\right)+\bar{\pi}\frac{\vartheta_2+1+\vartheta_2 t}{\vartheta_2+1}\exp\left(-\vartheta_2 t\right)}. \tag{38}$$

where $R\left(t|\breve{\Delta}\right)$ is given in Eq (28).

4. Estimation inference via simulation

Several statistical characteristics of the 2-CMLM $\left(\breve{\Delta}\right)$ are contributed to this section, considering that parametric vector $\breve{\Delta}$ is unknown. The assessment of parametric vector $\breve{\Delta}$ is carried out by the three well known estimation methods such as maximum likelihood estimation, Least square Estimation (LSE) and Weighted Least square Estimation (WLSE). From now, $t_1,t_2,...,t_n$ represent n observed values from T and their ascending ordering values $t_{(1)}\le t_{(2)}\le ...\le t_{(n)}$.

4.1. Maximum likelihood estimation (MLE)

The most widely known approach of parameter estimate is the maximum likelihood method. The method's popularity is due to its numerous desired qualities, such as consistency, normality and asymptotic efficiency. Let $t_1,t_2,...,t_n$ be n observed values from the Eq (2) and $\breve{\Delta}$ be the vector of unknown parameters. The assessments of MLEs of $\breve{\Delta}$ can be provided by optimizing the likelihood function with respect to ϑ_1, ϑ_2, and π given by $L\left(\mathbf{t}|\breve{\Delta}\right)=\prod_{i=1}^{n}f\left(t_i;\breve{\Delta}\right)$ or likewise the log-likelihood function for $\breve{\Delta}$ given by

$$l\left(\mathbf{t}|\breve{\Delta}\right)=\ln\prod_{i=1}^{n}f\left(t_i;\breve{\Delta}\right) \tag{39}$$

$$l\left(\mathbf{t}|\breve{\Delta}\right)=\sum_{i=1}^{n}\ln\left\{\pi\frac{\vartheta_1^2}{\vartheta_1+1}\left(1+t_i\right)\exp\left(-\vartheta_1 t_i\right)+\bar{\pi}\frac{\vartheta_2^2}{\vartheta_2+1}\left(1+t_i\right)\exp\left(-\vartheta_2 t_i\right)\right\}. \tag{40}$$

So, by partially differentiating $l\left(\mathbf{t}|\breve{\Delta}\right)$ with regard to each of the parameters $\left(\vartheta_1,\vartheta_2,\pi\right)$ and setting the findings to zero, the MLEs of the respective parameters are obtained, the likelihood equations are

$$\frac{\partial l\left(\mathbf{t}|\breve{\Delta}\right)}{\partial\vartheta_1}=\sum_{i=1}^{n}\frac{\pi\left(1+t_i\right)\left\{\frac{2\vartheta_1\exp\left(-\vartheta_1 t_i\right)}{\left(\vartheta_1+1\right)}-\frac{\vartheta_1^2 t_i\exp\left(-\vartheta_1 t_i\right)}{\left(\vartheta_1+1\right)}-\frac{\vartheta_1^2\exp\left(-\vartheta_1 t_i\right)}{\left(\vartheta_1+1\right)^2}\right\}}{\left\{\pi\frac{\vartheta_1^2}{\vartheta_1+1}\left(1+t_i\right)\exp\left(-\vartheta_1 t_i\right)+\bar{\pi}\frac{\vartheta_2^2}{\vartheta_2+1}\left(1+t_i\right)\exp\left(-\vartheta_2 t_i\right)\right\}}, \tag{41}$$

$$\frac{\partial l\left(\mathbf{t}|\breve{\Delta}\right)}{\partial\vartheta_2}=\sum_{i=1}^{n}\frac{\pi\left(1+t_i\right)\left\{\frac{2\vartheta_2\exp\left(-\vartheta_2 t_i\right)}{\left(\vartheta_2+1\right)}-\frac{\vartheta_2^2 t_i\exp\left(-\vartheta_2 t_i\right)}{\left(\vartheta_2+1\right)}-\frac{\vartheta_2^2\exp\left(-\vartheta_2 t_i\right)}{\left(\vartheta_2+1\right)^2}\right\}}{\left\{\pi\frac{\vartheta_1^2}{\vartheta_1+1}\left(1+t_i\right)\exp\left(-\vartheta_1 t_i\right)+\bar{\pi}\frac{\vartheta_2^2}{\vartheta_2+1}\left(1+t_i\right)\exp\left(-\vartheta_2 t_i\right)\right\}}, \tag{42}$$

$$\frac{\partial l\left(\mathbf{t}|\breve{\Delta}\right)}{\partial\pi}=\sum_{i=1}^{n}\frac{\frac{\vartheta_1^2}{\vartheta_1+1}\left(1+t_i\right)\exp\left(-\vartheta_1 t_i\right)-\frac{\vartheta_2^2}{\vartheta_2+1}\left(1+t_i\right)\exp\left(-\vartheta_2 t_i\right)}{\left\{\pi\frac{\vartheta_1^2}{\vartheta_1+1}\left(1+t_i\right)\exp\left(-\vartheta_1 t_i\right)+\bar{\pi}\frac{\vartheta_2^2}{\vartheta_2+1}\left(1+t_i\right)\exp\left(-\vartheta_2 t_i\right)\right\}}. \tag{43}$$

As a result, solving this nonlinear system of equations gives the MLE. Although these equations cannot be analytically solved, we use statistical software through iterative approach like Newton method or fixed point iteration methods can be used to solve them.

4.2. Least square estimators (LSE)

For estimating unknown parameters, the ordinary least square approach is well-known [36]. The least square estimators of ϑ_1, ϑ_2 and π denoted by $\tilde{\vartheta}_{1_{LSE}}, \tilde{\vartheta}_{2_{LSE}}$ and $\tilde{\pi}_{LSE}$, can be obtained by minimizing the function

$$LS(\breve{\Delta}) = \sum_{i=1}^{n}\left[F\left(t_{(i)}\middle|\breve{\Delta}\right) - \frac{i}{n+1}\right]^2, \tag{44}$$

with respect to ϑ_1, ϑ_2 and π where $F(\ )$ is given by Eq (4). They can be derived in the same way by solving the following nonlinear equations:

$$\frac{\partial LS(\breve{\Delta})}{\partial \vartheta_1} = \sum_{i=1}^{n}\left[F\left(t_{(i)}\middle|\breve{\Delta}\right) - \frac{i}{n+1}\right]\breve{\Psi}_1\left(t_{(i)}\middle|\vartheta_1\right) = 0, \tag{45}$$

$$\frac{\partial LS(\breve{\Delta})}{\partial \vartheta_2} = \sum_{i=1}^{n}\left[F\left(t_{(i)}\middle|\breve{\Delta}\right) - \frac{i}{n+1}\right]\breve{\Psi}_2\left(t_{(i)}\middle|\vartheta_2\right) = 0, \tag{46}$$

and

$$\frac{\partial LS(\breve{\Delta})}{\partial \pi} = \sum_{i=1}^{n}\left[F\left(t_{(i)}\middle|\breve{\Delta}\right) - \frac{i}{n+1}\right]\breve{\Psi}_3\left(t_{(i)}\middle|\pi\right) = 0, \tag{47}$$

where

$$\breve{\Psi}_1\left(t_{(i)}\middle|\vartheta_1\right) = \pi\frac{t_{(i)}\vartheta_1\exp\left(-\vartheta_1 t_{(i)}\right)\left(2+t_{(i)}+\vartheta_1+t_{(i)}\vartheta_1\right)}{\left(\vartheta_1+1\right)^2}, \tag{48}$$

$$\breve{\Psi}_2\left(t_{(i)}\middle|\vartheta_2\right) = \breve{\pi}\frac{t_{(i)}\vartheta_2\exp\left(-\vartheta_2 t_{(i)}\right)\left(2+t_{(i)}+\vartheta_2+t_{(i)}\vartheta_2\right)}{\left(\vartheta_2+1\right)^2}, \tag{49}$$

$$\breve{\Psi}_3\left(t_{(i)}\middle|\pi\right) = \frac{\exp\left(-\vartheta_2 t_{(i)}\right)\left(1+\vartheta_2+\vartheta_2 t_{(i)}\right)}{\left(\vartheta_2+1\right)} - \frac{\exp\left(-\vartheta_1 t_{(i)}\right)\left(1+\vartheta_1+t_{(i)}\vartheta_1\right)}{\left(\vartheta_1+1\right)}. \tag{50}$$

4.3. Weighted Least Squares Estimators (WLSE)

Consider the weighted function below (see [37])

$$\kappa_i = \frac{(n+1)^2(n+2)}{i(n-i+1)}. \tag{51}$$

The WLSEs $\tilde{\vartheta}_{1_{WLSE}}, \tilde{\vartheta}_{2_{WLSE}}$ and $\tilde{\pi}_{WLSE}$ can be obtained by minimizing the function

$$WLS\left(\breve{\Delta}\right) = \sum_{i=1}^{n} \frac{(n+1)^2(n+2)}{i(n-i+1)} \left[F\left(t_{(i)} \middle| \breve{\Delta}\right) - \frac{i}{n+1} \right]^2, \tag{52}$$

One can also get these estimators by solving:

$$\frac{\partial WLS(\breve{\Delta})}{\partial \vartheta_1} = \sum_{i=1}^{n} \frac{(n+1)^2(n+2)}{i(n-i+1)} \left[F\left(t_{(i)} \middle| \breve{\Delta}\right) - \frac{i}{n+1} \right] \breve{\Psi}_1\left(t_{(i)} \middle| \vartheta_1\right) = 0, \tag{53}$$

$$\frac{\partial WLS(\breve{\Delta})}{\partial \vartheta_2} = \sum_{i=1}^{n} \frac{(n+1)^2(n+2)}{i(n-i+1)} \left[F(t_{(i)} \middle| \breve{\Delta}) - \frac{i}{n+1} \right] \breve{\Psi}_2\left(t_{(i)} \middle| \vartheta_2\right) = 0, \tag{54}$$

and

$$\frac{\partial WLS(\breve{\Delta})}{\partial \pi} = \sum_{i=1}^{n} \frac{(n+1)^2(n+2)}{i(n-i+1)} \left[F\left(t_{(i)} \middle| \breve{\Delta}\right) - \frac{i}{n+1} \right] \breve{\Psi}_3\left(t_{(i)} \middle| \pi\right) = 0, \tag{55}$$

where $\breve{\Psi}_1\left(t_{(i)} \middle| \vartheta_1\right)$, $\breve{\Psi}_2\left(t_{(i)} \middle| \vartheta_2\right)$ and $\breve{\Psi}_3\left(t_{(i)} \middle| \pi\right)$ are given in Eqs (48–50).

5. Simulation study

We use the simulation to analyze various estimating strategies that were discussed in subsection 4.1–4.3. As a result, we execute some Monte Carlo simulations with various mixing proportions π and model parameters. Three simulation experiments are used in order to assess the performance of MLE, performance, LSEs and WLSEs of the 2-CMLM $\left(\breve{\Delta}\right)$ parameters. The bias and MSE measures are used to discuss the precision of the MLEs, LSEs and WLSEs. The efficiency of each parameter estimation approach for the 2-CMLM $\left(\breve{\Delta}\right)$ model in terms of n is considered. The steps of the simulation algorithm are as follows:

1. By varying the mixing proportion π and the model parameters $(\pi, \vartheta_1, \vartheta_2) = (0.4, 0.65, 0.6), (0.6, 0.25, 0.27)$ and $(0.9, 0.12, 0.15)$, generate random samples of sizes $10,13,...,300$ from the 2-CMLM $\left(\breve{\Delta}\right)$. The simulation's random samples are generated as described in the next stage.
2. Using the R uniform generator (runif), create one variate *u* from the uniform distribution $U(0,1)$.
3. If $u \le \pi$, we use the (*rlindley*) function to generate a random variate from the first component, which is a Lindley distribution (ϑ_1). If $u > \pi$, the second component, a Lindley distribution (ϑ_2), is used to generate a random variate.
4. Begin to (2) until the required sample of size n is obtained.
5. Using 1000 replications, repeat steps 1–4 again. Compute the MLEs, LSEs and WLSEs for the

1000 samples; say $\breve{\theta}_j$ for $j=1,2,...,1000$, using the optima function and the Nelder-Mead technique in R to calculate the estimator values. The simulated densities for three parametric sets are shown in Figure 8.

6. Calculate biases and MSEs. These objectives are obtained with the help of the following formulas:

$$Bias_{\theta}(n)=\frac{1}{1000}\sum_{j=1}^{1000}\left(\breve{\theta}_j-\theta\right), \tag{56}$$

$$MSE_{\theta}(n)=\frac{1}{1000}\sum_{j=1}^{1000}\left(\breve{\theta}_j-\theta\right)^2, \tag{57}$$

where $\theta=(\vartheta_1,\vartheta_2,\pi)$.

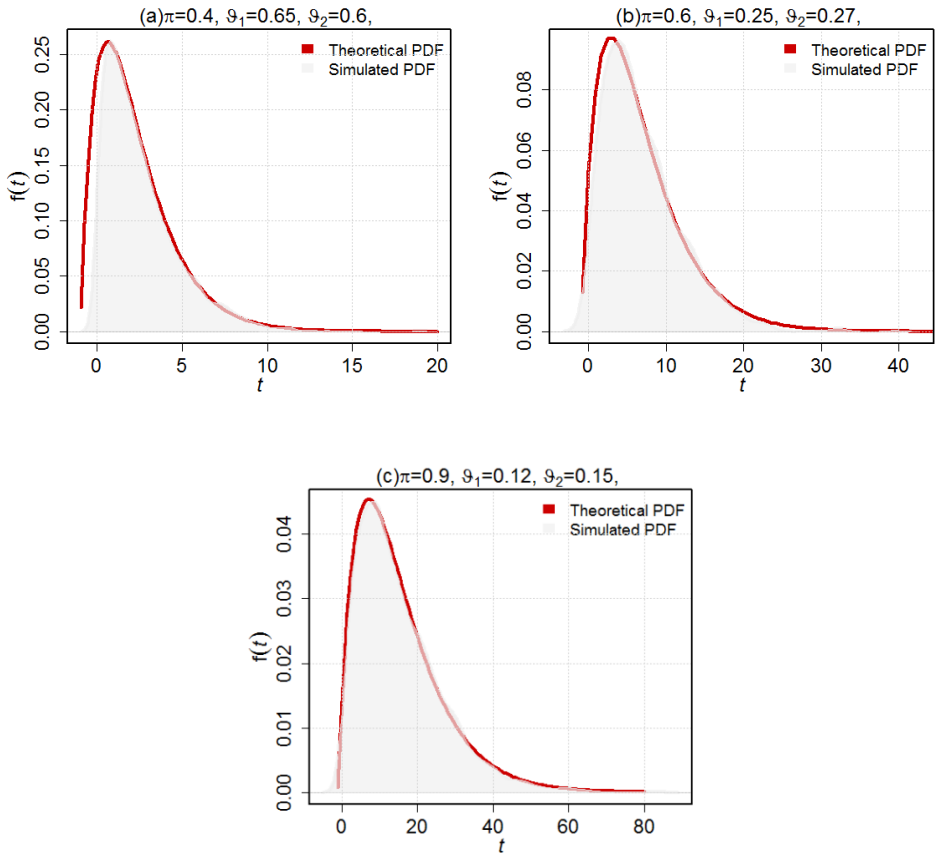

Figure 8. The simulated densities for three parameter vectors.

The results of simulation study of this subsection are indicated in Figures 9–14. These empirical findings show that the proposed estimate methods do a good job of estimating the 2-CMLM $\left(\breve{\Delta}\right)$ parameters. Because the bias tends to zero as n increases, we can deduce that the estimators exhibit the attribute of asymptotic unbiasedness. The mean squared error behavior, on the other hand, indicates consistency because the errors tend to zero as n increases. From Figures 9–14, the following observations can be extracted.

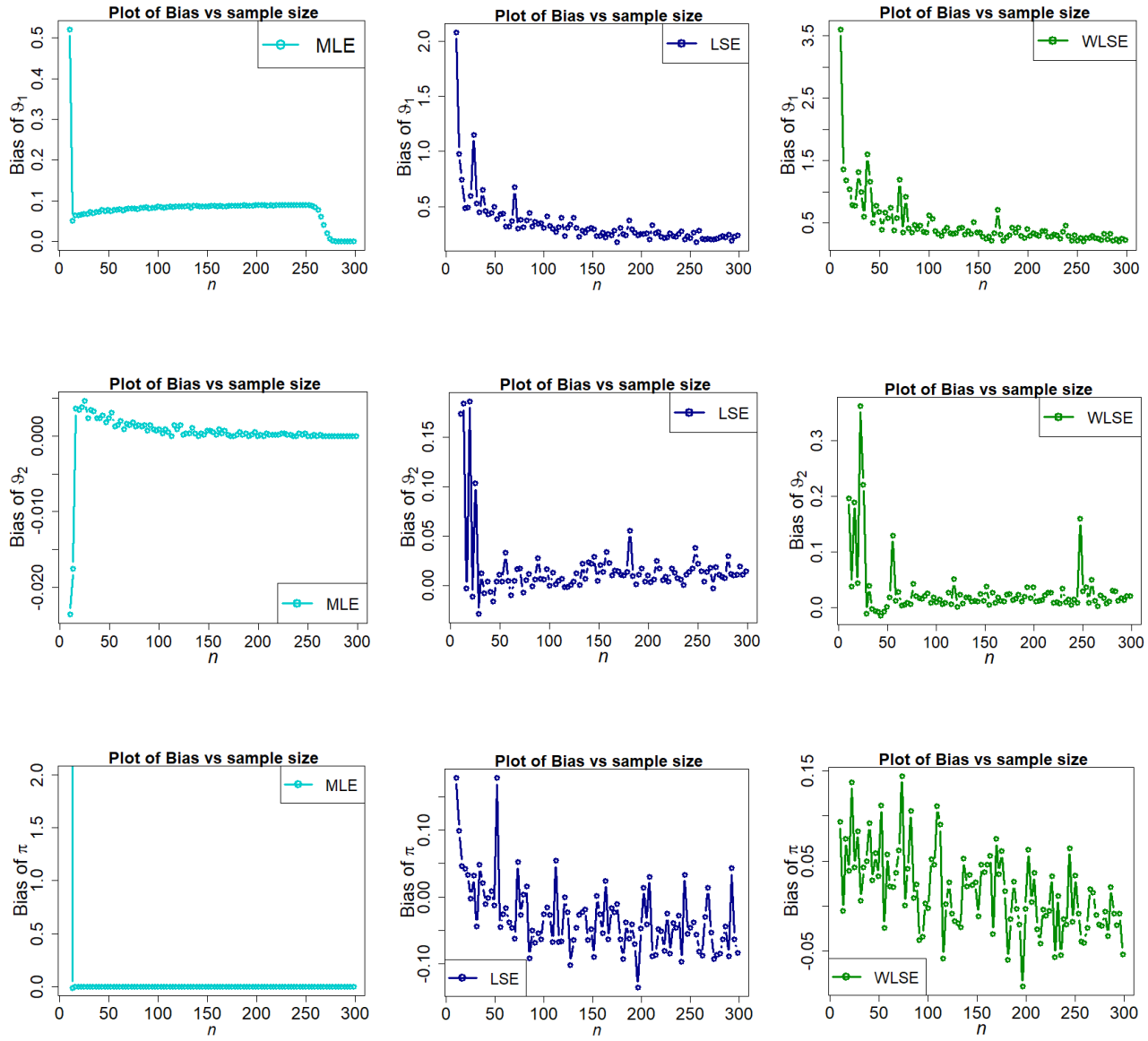

Figure 9. Fluctuations of bias of $\breve{\vartheta}_1, \breve{\vartheta}_2, \breve{\pi}$ under different methods of estimation for parametric set I.

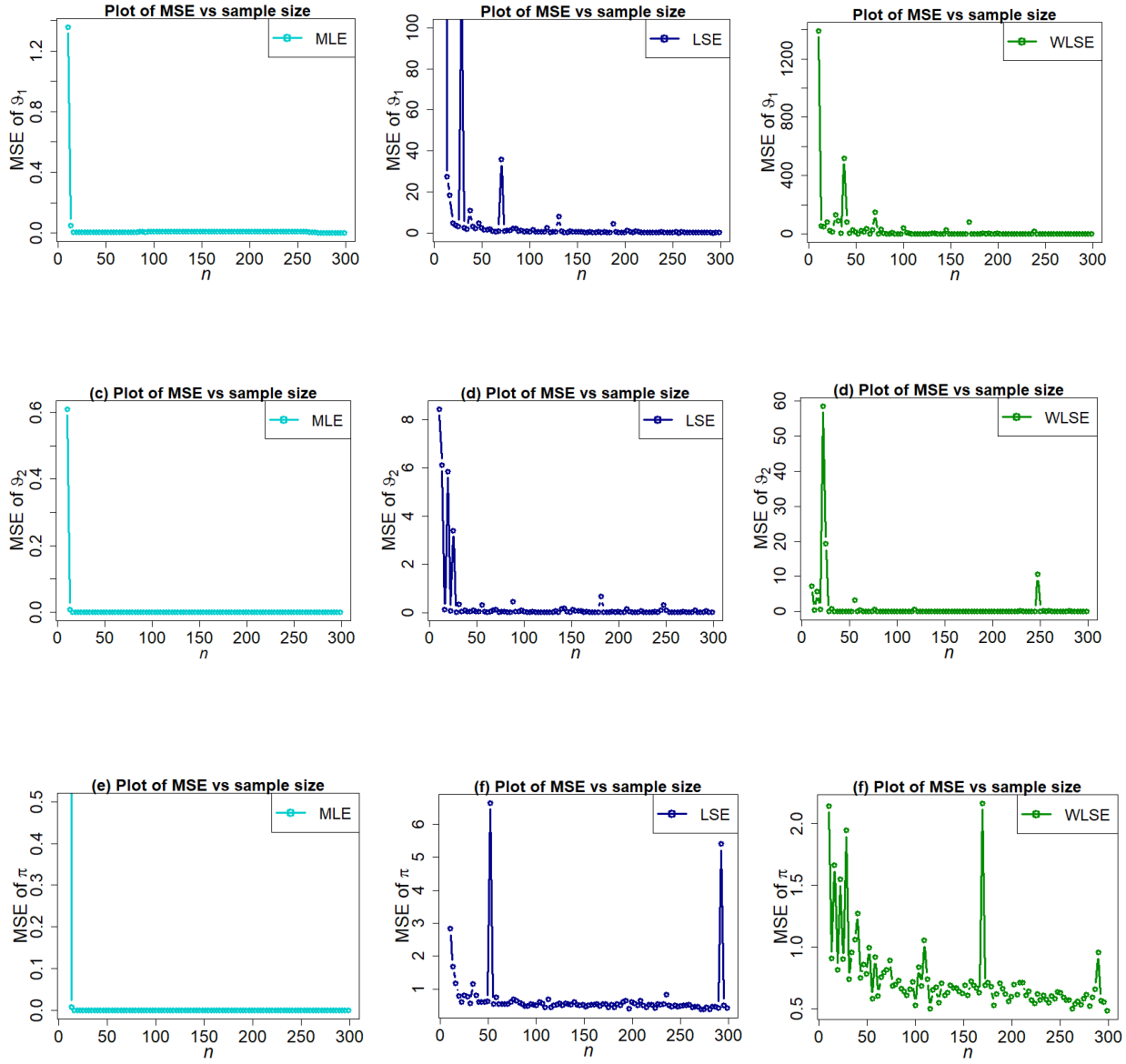

Figure 10. Fluctuations of MSE of $\breve{\vartheta}_1, \breve{\vartheta}_2, \breve{\pi}$ under different methods of estimation for parametric set I.

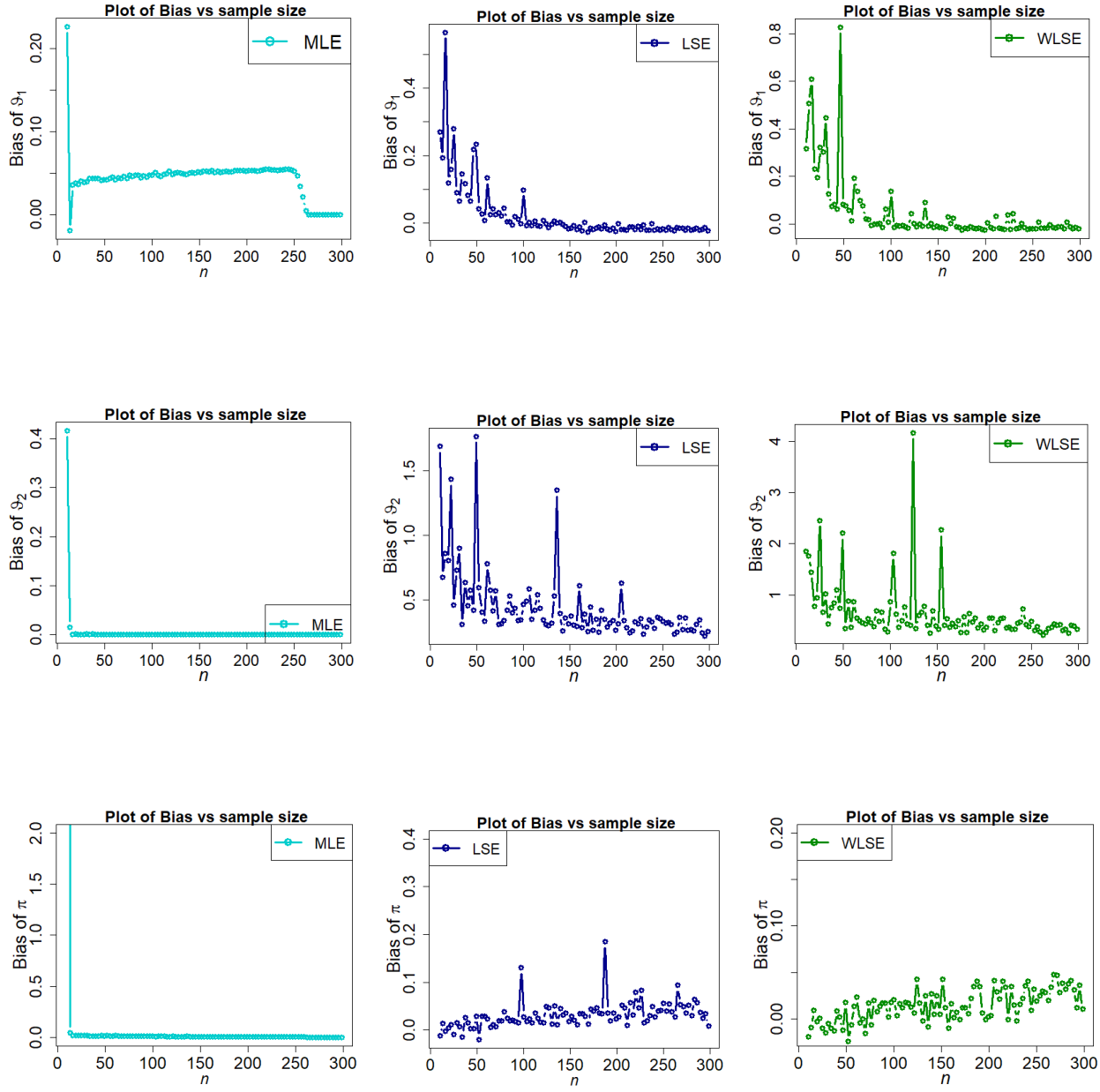

Figure 11. Fluctuations of bias of $\breve{\vartheta}_1, \breve{\vartheta}_2, \breve{\pi}$ under different methods of estimation for parametric set II.

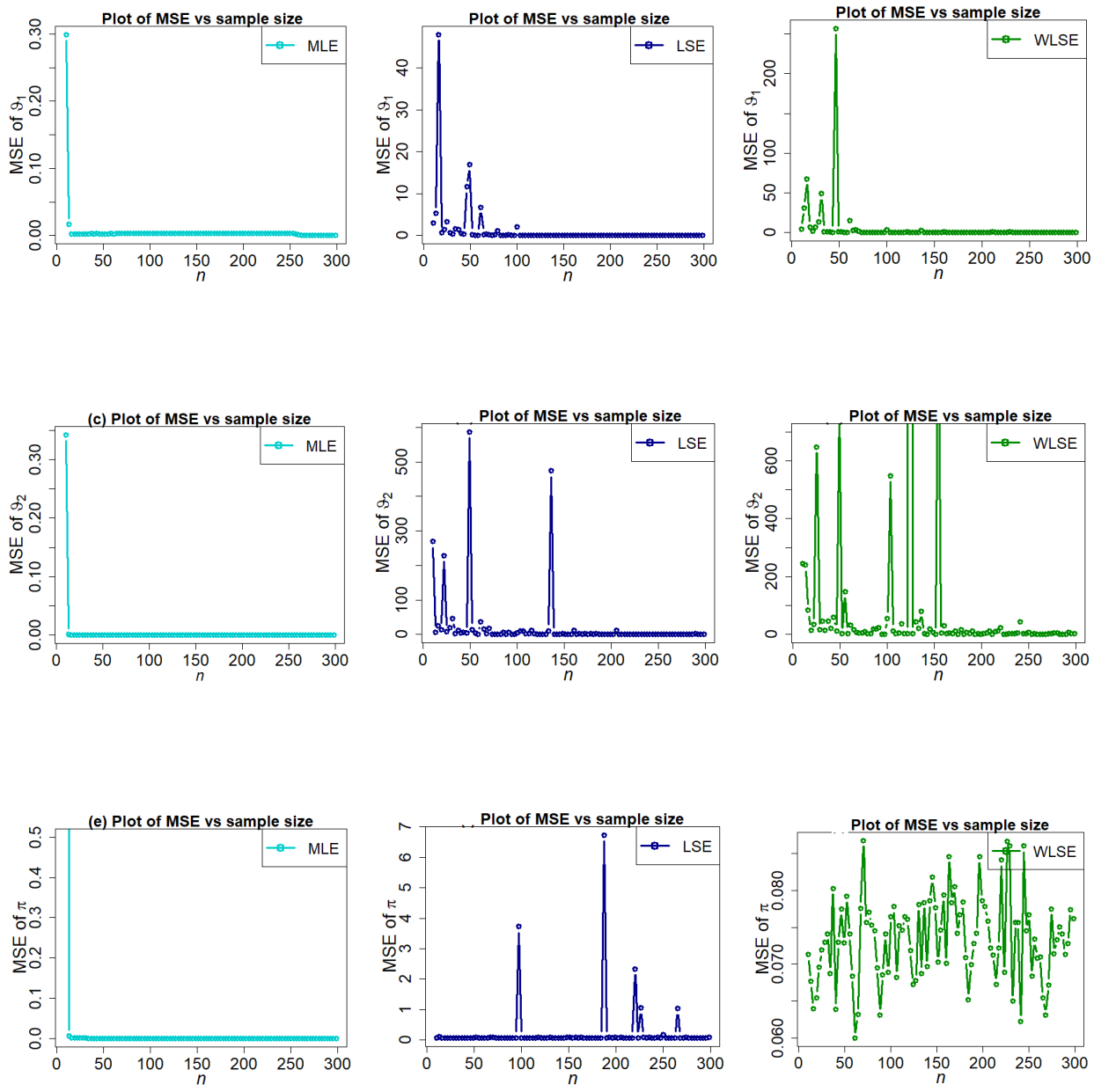

Figure 12. Fluctuations of MSE of $\breve{\vartheta}_1, \breve{\vartheta}_2, \breve{\pi}$ under different methods of estimation for parametric set II.

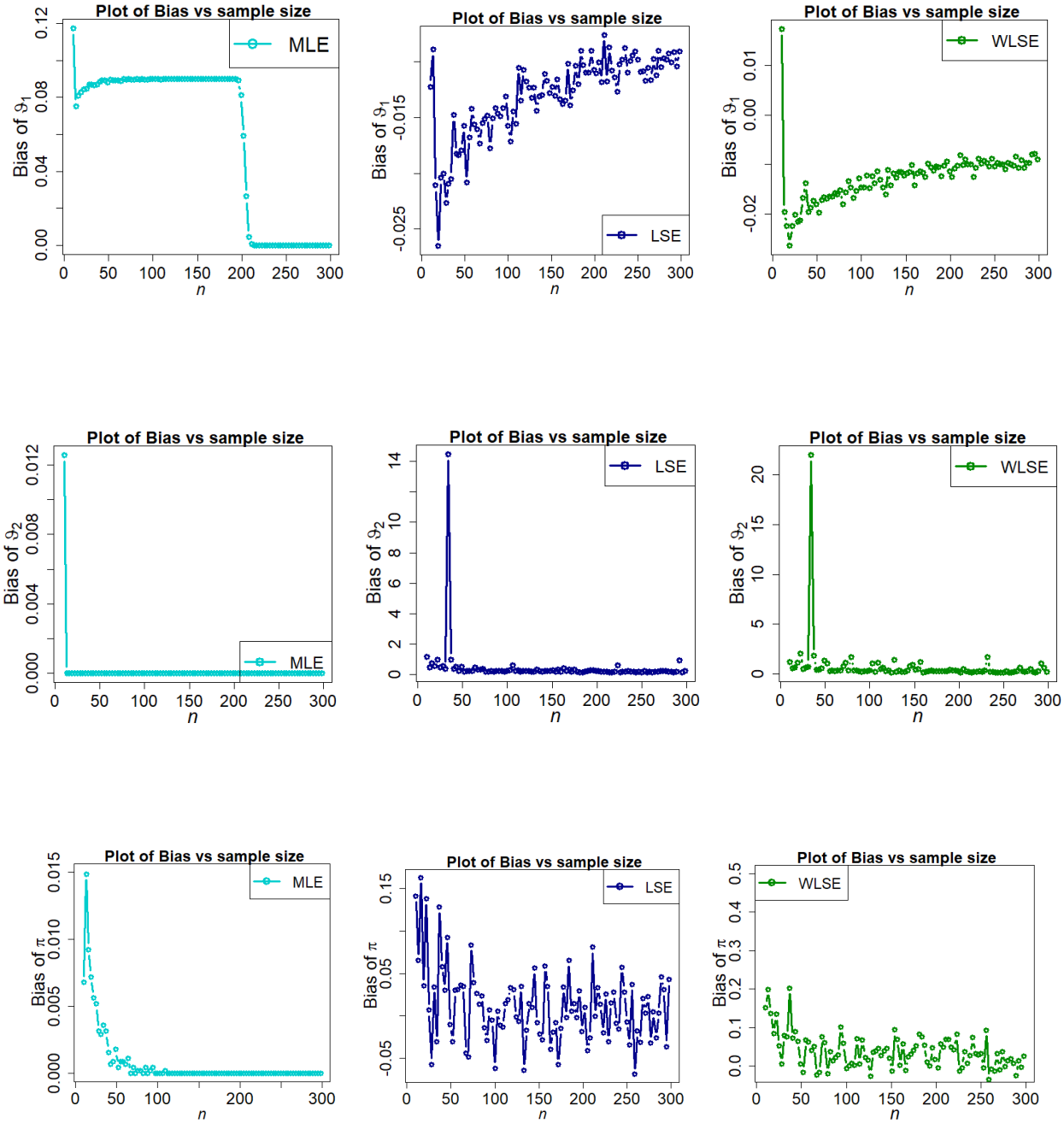

Figure 13. Fluctuations of bias of $\breve{\vartheta}_1, \breve{\vartheta}_2, \breve{\pi}$ under different methods of estimation for parametric set III.

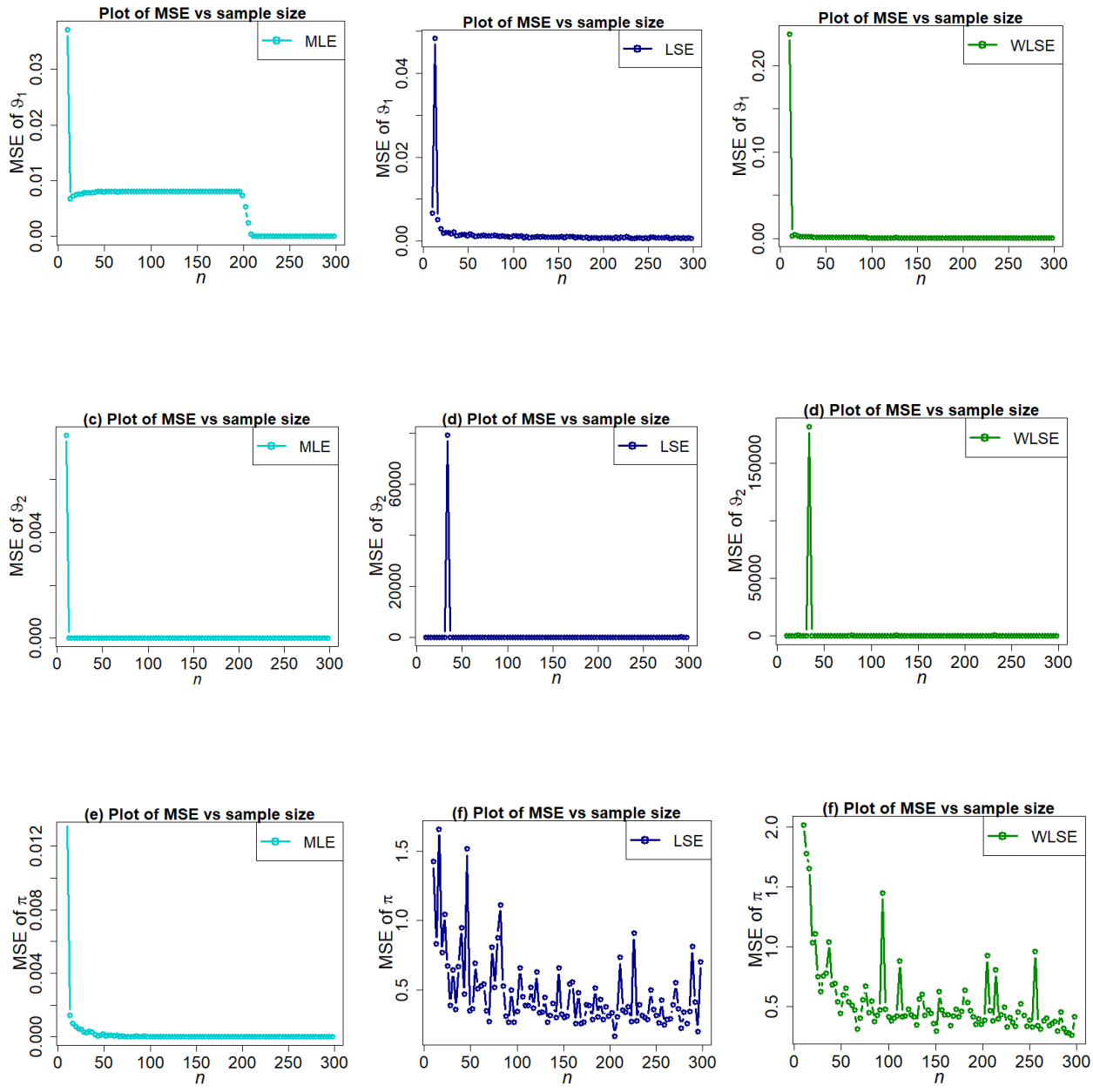

Figure 14. Fluctuations of MSE of $\breve{\vartheta}_1, \breve{\vartheta}_2, \breve{\pi}$ under different methods of estimation for parametric set III.

- The estimated bias of parameters $\breve{\vartheta}_1, \breve{\vartheta}_2, \breve{\pi}$, decreases as n increases under all estimation approaches.
- From Figure 9 for parametric Set-I, we can see that the estimated bias of parameters ϑ_1 and π is over-estimated in all three estimation methods while ϑ_2 is under estimated in MLE.
- From Figure 13 for parametric Set-III, we can see that the estimated bias of parameters ϑ_1 and π is under-estimated in LSE estimation method and ϑ_1 over-estimated in WLSE estimation method while ϑ_2 is over-estimated in all three estimation methods.
- The estimated bias of parameters $\vartheta_1, \vartheta_2, \pi$ is over-estimated in both estimation methods for parametric Set-II (see Figure 11).

- In terms of bias, generally the performances of the MLE, is the good (see Figures 9, 11and 13).
- Furthermore, Figures 10, 12 and 14 show that the MSE for MLE, LSE and WLSE estimate methods reduces as n increases, satisfying the consistency criterion.
- Under all estimation procedures, the difference between estimates and assumed parameters decreases to zero as sample size increases.
- When the sample size approaches infinity, MLE estimation is often stronger in terms of bias and MSE when compared to alternative estimation techniques for all stated parameter values (see Figures 9–14).

The basic conclusion from the previous figures is that as the sample size grows the estimated bias and MSE graphs for parameters ϑ_1, ϑ_2 and π eventually approach zero for all estimation methods. This validates the accuracy of these estimation approaches, as well as the numerical computations for the 2-CMLM $\left(\breve{\Delta}\right)$ parameters.

6. Applications to COVID-19 data

The major purpose of the 2-CMLM $\left(\breve{\Delta}\right)$ distribution's derivation is to employ it in data analysis purposes, which makes it valuable in a variety of domains, notably those dealing with lifetime analysis. This section demonstrates how the 2-CMLM $\left(\breve{\Delta}\right)$ works by applying the suggested model to real-world data. This aspect is demonstrated here by comparing two sets of data from COVID-19 pandemic outbreaks. [38–43] also studied the COVID-19 datasets to fit the new distribution. The given data sets are used to compare the fit of the 2-CMLM $\left(\breve{\Delta}\right)$ to a competing model that is a two component mixture of exponential models (2-CMEM $\left(\breve{\Delta}\right)$) and two component mixture of Weibull models (2-CMWM $\left(\breve{\Delta}\right)$) by using R function maxLik (.). We demonstrate that the 2-CMLM $\left(\breve{\Delta}\right)$ provides great fit to the COVID-19 pandemic lifespan data. The concept "best fit" refers to the proposed model having lower values for the measure chosen for comparison.-Log-likelihood $(-LL)$ the AIC (Akaike information criterion), the BIC (Bayesian information criterion), and the CAIC (Corrected Akaike information criterion) are some of the discriminatory measures/goodness-of-fit (GoF) incorporated in these criteria. The best model for the real data set might be the one with the lowest values of the above-mentioned measures.

DataSet-1: The data represents a COVID-19 data belong to Italy of 59 days that is recorded from 27 February to 27 April 2020. This data formed of rough mortality rate. This data set can be accessed at https://covid19.who.int/.

DataSet-2: We investigate the survival times of people in China who have been infected with the COVID-19 virus. The data set under consideration represents patient survival times from the moment they were admitted to the hospital until they deceased. https://www.worldometers.info/coronavirus/ can be used to access the data set. This data is used in [44].

The MLEs of the 2-CMLM$\left(\breve{\Delta}\right)$ and Goodness-of-Fit measures are provided in Tables 1and 2. The outcomes of these Tables clearly show that the 2-CMLM$\left(\breve{\Delta}\right)$ is the best of 2-CMLM$\left(\breve{\Delta}\right)$ as it has the smaller values of the -LL, AIC, BIC, and CAIC. In comparison 2-CMLM$\left(\breve{\Delta}\right)$ the 2-CMLM $\left(\breve{\Delta}\right)$ provides a very good fit for these data, as seen in the Tables. According to dataset one,

2-CMWM has the smallest -LL, as well as the smallest AIC, the BIC, and the CAIC. But if we consider the mixture of two parsimonious models 2-CMLM perform well. The best distribution for fitting the dataset II is 2-CMLM, as seen in Table 2 because the 2-CMLM model has the smallest AIC, the BIC, and the CAIC even though -LL is little bit high as compare to 2-CMWM but most Goodness-of-Fit measures are in favor of 2-CMLM model. So, the best distribution for fitting the dataset II is 2-CMLM, as seen in Figure 15.

Figures 15 and 16 depict probability-probability (P-P) plots for 2-CMLM$\left(\breve{\Delta}\right)$ and 2-CMEM$\left(\breve{\Delta}\right)$ and for 2-CMWM$\left(\breve{\Delta}\right)$ respectively, which support the findings of Tables 1 and 2. Figures 17 and 18 show the profiles of the log-likelihood function (PLLF) based on data sets.

Table 1. MLEs and Goodness-of-Fit statistics for the Dataset I.

Distributions		MLEs	-LL	AIC	BIC	CAIC
2-CMLM	$\breve{\vartheta}_1$	0.22286	−173.2998	352.5996	358.8322	353.036
	$\breve{\vartheta}_2$	0.22290				
	$\breve{\pi}$	0.38676				
2-CMEM	$\breve{\vartheta}_1$	0.12253	−182.8277	371.6554	377.888	372.0918
	$\breve{\vartheta}_2$	0.12261				
	$\breve{\pi}$	0.23042				
2-CMWM	$\breve{\vartheta}_1$	4.47462	−167.701	331.4109	341.7987	332.5431
	$\breve{\vartheta}_2$	3.95049				
	$\breve{\vartheta}_3$	3.15885				
	$\breve{\vartheta}_4$	11.8225				
	$\breve{\pi}$	0.34695				

Table 2. MLEs and Goodness-of-Fit statistics for the Dataset II.

Distributions		MLEs	-LL	AIC	BIC	CAIC
2-CMLM	$\breve{\vartheta}_1$	2.19355	−131.585	269.170	273.9206	269.6598
	$\breve{\vartheta}_2$	0.25458				
	$\breve{\pi}$	0.35147				
2-CMEM	$\breve{\vartheta}_1$	0.16157	−131.8065	269.613	274.3636	270.1028
	$\breve{\vartheta}_2$	1.87025				
	$\breve{\pi}$	0.75191				
2-CMWM	$\breve{\vartheta}_1$	2.7244	−130.874	271.7481	281.5995	273.0246
	$\breve{\vartheta}_2$	0.6754				
	$\breve{\vartheta}_3$	0.8915				
	$\breve{\vartheta}_4$	5.5149				
	$\breve{\pi}$	0.1912				

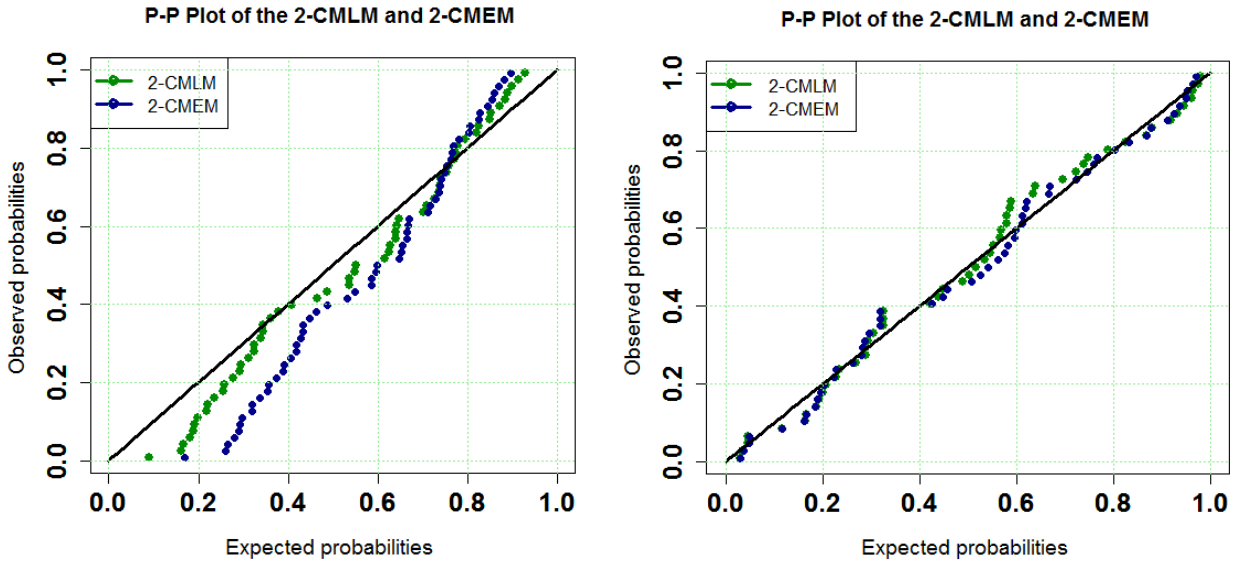

Figure 15. The PP plots for Datasets I and II.

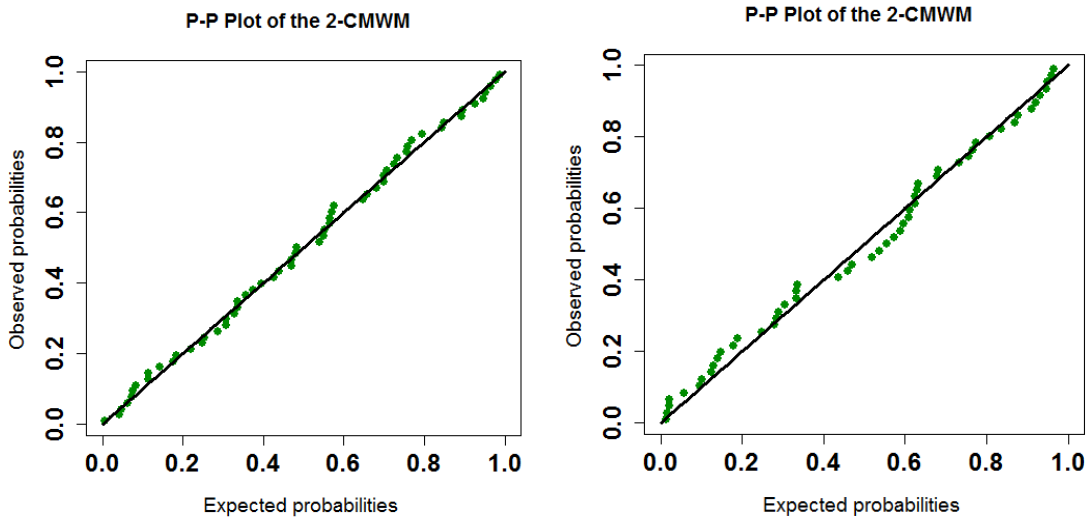

Figure 16. The PP plots of 2-CMWM for Datasets I and II.

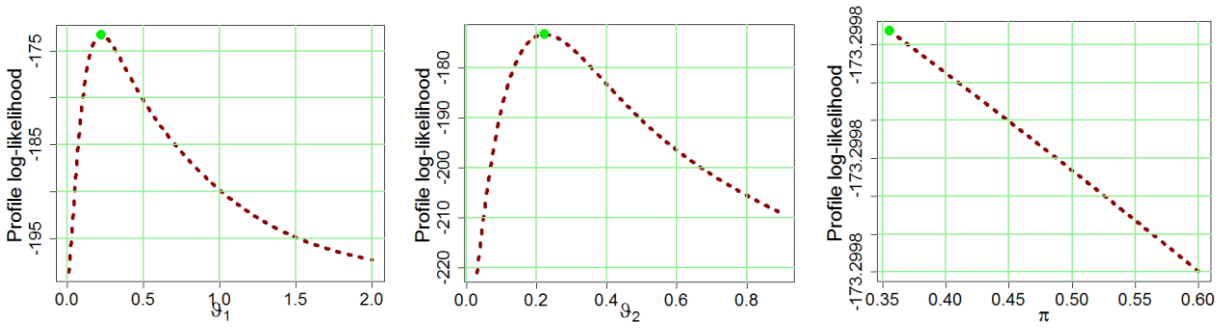

Figure 17. The profile of the log-likelihood function for Dataset I.

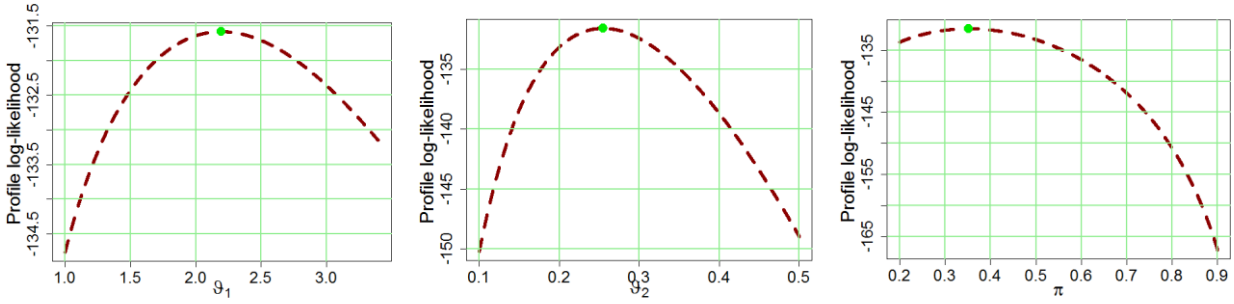

Figure 18. The profile of the log-likelihood function for Dataset II.

7. Conclusions

We studied two component mixture of Lindley models in this study using three estimate techniques: MLE, LSE, and WLSE. Further, some additional statistical and reliability properties of the two Lindley mixture model were obtained, like central moments, Cumulants, Cumulant Generating Function, Probability Generating Function, Factorial Moment Generating Function, Coefficient of variation, skewness and kurtosis, Mills Ratio, Reversed Hazard Rate Function, Mean Time to Failure, and Mean Residual Life. A simulation study was conducted using 1000 replications to explore and compare the performance of the estimation techniques. As a consequence, we found that the ML technique outperformed the others in terms of accuracy and consistency when estimating model unknown parameters. Moreover, to demonstrate the usefulness of the underlying mixture model, we used some real dataset. We demonstrated that the Lindley mixture model is suitable and effective for data modelling, and that it outperforms the exponential mixture model, using two real datasets.

Acknowledgment

The authors extend their appreciation to the Deanship of Scientific Research at King Khalid University, Abha, Saudi Arabia for funding this work through research groups program under grant number RGP.2/120/42. The authors would like to thank the Editor and anonymous reviewers for their constructive comments that improved the final version of the paper.

Conflict of interest

There is no conflict of interest declared by the authors.

References

1. B. S. Everitt, A finite mixture model for the clustering of mixed-mode data, *Stat. Probabil. Lett.*, **6** (1988), 305–309. https://doi.org/10.1016/0167-7152(88)90004-1
2. B. G. Lindsay, Mixture models: Theory, geometry and applications. In: NSF-CBMS regional conference series in probability and statistics (pp. i-163), Institute of Mathematical Statistics and the American Statistical Association, 1995, January. https://doi.org/10.1214/cbms/1462106013
3. G. J. McLachlan, K. E. Basford, Mixture models: Inference and applications to clustering, New York: M. Dekker, **38** (1988). https://doi.org/10.2307/2348072
4. G. McLachlan, D. Peel, Finite Mixture Models, John Wiley & Sons: New York, 2000. https://doi.org/10.1002/0471721182
5. J. Q. Shi, R. Murray-Smith, D. M. Titterington, Bayesian regression and classification using mixtures of Gaussian processes, *Int. J. Adapt. Control.*, **17** (2003), 149–161. https://doi.org/10.1002/acs.744
6. D. Mohammad, A. Muhammad, On the Mixture of BurrXII and Weibull Distribution, *J. Sta. Appl. Pro*, **3** (2014), 251–267. https://doi.org/10.12785/jsap/030215
7. K. S. Sultan, M. A. Ismail, A. S. Al-Moisheer, Mixture of two inverse Weibull distributions: Properties and estimation, *Comput. Stat. Data An.*, **51** (2007), 5377–5387. https://doi.org/10.1016/j.csda.2006.09.016

8. R. Jiang, D. N. P. Murthy, P. Ji, Models involving two inverse Weibull distributions, *Reliab. Eng. Syst. Safe.,* **73** (2001), 73–81. https://doi.org/10.1016/S0951-8320(01)00030-8
9. A. Mohammadi, A. M. R. Salehi-Rad, E. C. Wit, Using mixture of Gamma distributions for Bayesian analysis in an M/G/1 queue with optional second service, *Computation. Stat.,* **28** (2013), 683–700. https://doi.org/10.1007/s00180-012-0323-3
10. S. F. Ateya, Maximum likelihood estimation under a finite mixture of generalized exponential distributions based on censored data, *Stat. Pap.,* **55** (2014), 311–325. https://doi.org/10.1007/s00362-012-0480-z
11. M. M. Mohamed, E. Saleh, S. M. Helmy, Bayesian prediction under a finite mixture of generalized exponential lifetime model, *Pak. J. Stat. Oper. Res.,* (2014), 417–433. https://doi.org/10.18187/pjsor.v10i4.620
12. T. N. Sindhu, M. Aslam, Preference of prior for Bayesian analysis of the mixed Burr type X distribution under type I censored samples, *Pak. J. Stat. Oper. Res.,* (2014), 17–39. https://doi.org/10.18187/pjsor.v10i1.649
13. H. Zhang, Y. Huang, Finite mixture models and their applications: A review, *Austin Biom. Biostat.,* **2** (2015), 1–6.
14. T. N. Sindhu, M. Riaz, M. Aslam, Z. Ahmed, Bayes estimation of Gumbel mixture models with industrial applications, *T. I. Meas. Control,* **38** (2016), 201–214. https://doi.org/10.1177/0142331215578690
15. T. N. Sindhu, M. Aslam, Z. Hussain, A simulation study of parameters for the censored shifted Gompertz mixture distribution: A Bayesian approach, *J. Stat. Manag. Syst.,* **19** (2016), 423–450. https://doi.org/10.1080/09720510.2015.1103462
16. T. N. Sindhu, N. Feroze, M. Aslam, A. Shafiq, Bayesian inference of mixture of two Rayleigh distributions: A new look, *Punjab Univ. J. Math.,* **48** (2020).
17. T. N. Sindhu, H. M. Khan, Z. Hussain, B. Al-Zahrani, Bayesian inference from the mixture of half-normal distributions under censoring, *J. Natl. Sci. Found. Sri.,* **46** (2018), 587–600. https://doi.org/10.4038/jnsfsr.v46i4.8633
18. T. N. Sindhu, Z. Hussain, M. Aslam, Parameter and reliability estimation of inverted Maxwell mixture model, *J. Stat. Manag. Syst.,* **22** (2019), 459–493. https://doi.org/10.1080/09720510.2018.1552412
19. S. Ali, Mixture of the inverse Rayleigh distribution: Properties and estimation in a Bayesian framework, *Appl. Math. Modell.,* **39** (2015), 515–530. https://doi.org/10.1016/j.apm.2014.05.039
20. H. Zakerzadeh, A. Dolati, Generalized Lindley distribution, *J. Math. Ext.,* **3** (2009), 1–17.
21. B. O. Oluyede, T. Yang, A new class of generalized Lindley distributions with applications, *J. Stat. Comput. Sim.,* **85** (2015), 2072–2100. https://doi.org/10.1080/00949655.2014.917308
22. S. Nadarajah, H. S. Bakouch, R. Tahmasbi, A generalized Lindley distribution, *Sankhya B,* **73** (2011), 331–359. https://doi.org/10.1007/s13571-011-0025-9
23. D. V. Lindley, Bayesian statistics: A review, Society for industrial and applied mathematics, New York, United States, 1972. https://doi.org/10.1137/1.9781611970654.ch1
24. M. E. Ghitany, B. Atieh, S. Nadarajah, Lindley distribution and its application, *Math. Comput. Simulat.,* **78** (2008), 493–506. https://doi.org/10.1016/j.matcom.2007.06.007
25. R. Shanker, F. Hagos, S. Sujatha, On modeling of Lifetimes data using exponential and Lindley distributions, *Biometrics Biostatistics Int. J.,* **2** (2015), 1–9. https://doi.org/10.15406/bbij.2015.02.00042

26. J. Mazucheli, J. A. Achcar, The Lindley distribution applied to competing risks lifetime data, *Comput. Meth. Prog. Bio.*, **104** (2011), 188–192. https://doi.org/10.1016/j.cmpb.2011.03.006
27. D. K. Al-Mutairi, M. E. Ghitany, D. Kundu, Inferences on stress-strength reliability from Lindley distributions, *Commun. Stat.-Theory M.*, **42** (2013), 1443–1463. https://doi.org/10.1080/03610926.2011.563011
28. M. A. E. Damsesy, M. M. El Genidy, A. M. El Gazar, Reliability and failure rate of the electronic system by using mixture Lindley distribution, *J. Appl. Sci.*, **15** (2015), 524–530. https://doi.org/10.3923/jas.2015.524.530
29. A. H. Khan, T. R. Jan, Estimation of stress-strength reliability model using finite mixture of two parameter Lindley distributions, *J. Stat. Appl. Probab.*, **4** (2015), 147–159.
30. A. S. Al-Moisheer, A. F. Daghestani, K. S. Sultan, Mixture of two one-parameter Lindley distributions: properties and estimation, *J. Stat. Theory Pract.*, **15** (2021), 1–21. https://doi.org/10.1007/s42519-020-00133-4
31. S. Dey, D. Kumar, P. L. Ramos, F. Louzada, Exponentiated Chen distribution: properties and estimation, *Comm. Stat. Simul. C.*, **46** (2017), 8118–8139. https://doi.org/10.1080/03610918.2016.1267752
32. S. Dey, A. Alzaatreh, C. Zhang, D. Kumar, A new extension of generalized exponential distribution with application to ozone data, *Ozone Sci. Eng.*, **39** (2017), 273–285. https://doi.org/10.1080/01919512.2017.1308817
33. G. C. Rodrigues, F. Louzada, P. L. Ramos, Poisson exponential distribution: different methods of estimation, *J. Appl. Stat.*, **45** (2018), 128–144. https://doi.org/10.1080/02664763.2016.1268571
34. S. Dey, F. A. Moala, D. Kumar, Statistical properties and different methods of estimation of Gompertz distribution with application. *J. Stat. Manag. Syst.*, **21** (2018), 839–876. https://doi.org/10.1080/09720510.2018.1450197
35. S. Dey, M. J. Josmar, S. Nadarajah, Kumaraswamy distribution: different methods of estimation, *Comput. Appl. Math.*, **37** (2018), 2094–2111. https://doi.org/10.1007/s40314-017-0441-1
36. J. J. Swain, S. Venkatraman, J. R. Wilson, Least-squares estimation of distribution functions in Johnson's translation system, *J. Stat. Comput. Sim.*, **29** (1988), 271–297. https://doi.org/10.1080/00949658808811068
37. R. D. Gupta, D. Kundu, Generalized exponential distribution: different method of estimations, *J. Stat. Comput. Sim.*, **69** (2001), 315–337. https://doi.org/10.1080/00949650108812098
38. T. N. Sindhu, A. Shafiq, Q. M. Al-Mdallal, On the analysis of number of deaths due to Covid-19 outbreak data using a new class of distributions, *Results Phys.*, 21 (2021), 103747. https://doi.org/10.1016/j.rinp.2020.103747
39. T. N. Sindhu, A. Shafiq, Q. M. Al-Mdallal, Exponentiated transformation of Gumbel Type-II distribution for modeling COVID-19 data, *Alex. Eng. J.*, **60** (2021), 671–689. https://doi.org/10.1016/j.aej.2020.09.060
40. A. Shafiq, S. A. Lone, T. N. Sindhu, Q. M. Al-Mdallal, T. Muhammad, A New Modified Kies Fréchet Distribution: Applications of Mortality Rate of Covid-19, *Results Phys.*, (2021), 104638. https://doi.org/10.1016/j.rinp.2021.104638
41. S. A. Lone, T. N. Sindhu, F. Jarad, Additive Trinomial Fréchet distribution with practical application, *Results Phys.*, (2021), 105087. https://doi.org/10.1016/j.rinp.2021.105087

42. S. A. Lone, T. N. Sindhu, A. Shafiq, F. Jarad, A novel extended Gumbel Type II model with statistical inference and Covid-19 applications, *Results Phys.*, 35 (2022), 105377. https://doi.org/10.1016/j.rinp.2022.105377
43. A. Shafiq, T. N. Sindhu, N. Alotaibi, A novel extended model with versatile shaped failure rate: Statistical inference with Covid-19 applications, *Results Phys.*, 2022. https://doi.org/10.1016/j.rinp.2022.105398 https://doi.org/10.1016/j.rinp.2022.105398
44. X. Liu, Z. Ahmad, A. M. Gemeay, A. T. Abdulrahman, E. H. Hafez, N. Khalil, Modeling the survival times of the COVID-19 patients with a new statistical model: A case study from China, *Plos one*, **16** (2021), e0254999. https://doi.org/10.1371/journal.pone.0254999

AIMS Press